AMERICAN MUSEUM
Novitates

PUBLISHED BY THE AMERICAN MUSEUM OF NATURAL HISTORY
CENTRAL PARK WEST AT 79TH STREET, NEW YORK, N.Y. 10024
Number 3184, 43 pp., 19 figures, 8 tables November 22, 1996

Rhinocerotidae from the Middle Miocene of the Tung-gur Formation, Inner Mongolia (China)

ESPERANZA CERDEÑO[1]

CONTENTS

1. Postdoctoral Fulbright Scholar at the Department of Vertebrate Paleontology, American Museum of Natural History. Departamento de Paleobiología, Museo Nacional de Ciencias Naturales, José Gutiérrez Abascal, 2, 28006 Madrid, Spain.

ISSN 0003-0082 / Price $5.00

ABSTRACT

The rhinoceros material obtained by the old Central Asiatic Expeditions of the AMNH to Inner Mongolia (1928–1930) is studied herein. It was recovered from several sites within the Tung-gur Formation, of Middle Miocene age, which is correlated with the upper Aragonian (MN 8) of the European mammal biochronology. Three different species are recognized: one a member of the Aceratheriinae, *Acerorhinus zernowi*; one a member of the Rhinocerotinae of the subtribe Iranotheriina herein described as *Hispanotherium tungurense*, n. sp.; and one a Rhinocerotidae gen. and sp. indet., probably related to the Asian "*Dicerorhinus*." The taxonomy of both the acerathere and iranothere groups is discussed. Synonymies between *Acerorhinus* and *Hoploaceratherium* and between *Hispanotherium* and *Huaquingtherium* are proposed. The species *A. paleosinensis* and the "*A. incisivum*" from Tchobroutchi are removed from the genus *Acerorhinus*, being closer to *Chilotherium*. The species *G. mongoliense* is maintained within the genus *Gobitherium* and removed from *Iranotherium*. Phylogenetic relationships of these taxa are proposed by means of cladistic analysis.

INTRODUCTION

The fossiliferous Tung-gur sites of Inner Mongolia were discovered in 1928 during the Central Asiatic Expeditions of the American Museum of Natural History (AMNH). The fauna of the Tung-gur sites is currently recognized as characteristic of the East Asian Middle Miocene, which is correlated with the MN 8 biozone of the European Neogene (Qiu et al., 1988b; Qiu, 1990).

Recent studies of the Chinese Neogene mammalian faunas and biostratigraphy have led to a reinvestigation of such classical localities as Tung-gur. This work has uncovered new fossils, especially micromammals. Among perissodactyls, a member of the Rhinocerotidae, gen. and sp. indet., was reported (Qiu et al., 1988b; Qiu, 1990).

This paper deals with rhinoceros remains from Tung-gur housed at the AMNH since the 1930s. They were never published on, although Colbert (1939: 6) indicated the presence of *Aceratherium* among the Tung-gur fauna. These specimens were curated by Earl Manning, who identified the collections as containing *Iranotherium* cf. *longirhinus* and *Aceratherium*? cf. *depereti*. Two of Manning's notes (dated 1977–1978) refer to a comparison between "*Diceratherium*" *tsaidamense* Bohlin, 1937, and *Aceratherium depereti* Borissiak, 1927, concluding that the acerathere from Tung-gur is closer to the latter and suggesting a similarity with certain *Aphelops* from the Upper Ash Hollow Formation of Nebraska. Manning's notes also refer to differences between Tung-gur rhinos, "*Aceratherium*" (*Aphelops*?) and *Iranotherium*, in skull and dental features. A note with the collection of K. Heissig (dated 1985) indicates that there are several species within the *A.* cf. *depereti* set and that one of them seems to be *Aceratherium incisivum*.

MATERIAL AND METHODS

Besides their Tung-gur Formation origin, different localities are specified for the studied remains: Tairum Nor Basin, Gur Tung Khara Usu, *Platybelodon* Quarry, and Wolf Camp Quarry. Qiu et al. (1988b) explained that Tung-gur is apparently not a formal geographic name and that it corresponds to a well called Gur Tung Khara Usu, which corresponds to the well Donghuren Huduk. These authors established that the name Tung-gur is used to refer to the whole area where the Tung-gur Formation is exposed. Tairum Nor is placed at the southeast corner of the Tung-gur platform (Qiu et al., 1988b), and *Platybelodon* Quarry and Wolf Camp Quarry were working areas excavated during 1928–1930 (Osborn and Granger, 1932: fig. 1). Figure 1 shows the geography of the Tung-gur area.

MATERIAL

The available material (all from AMNH) is detailed for each mentioned locality and is referred to morphological type A (*Acerorhinus zernowi*), type B (*Hispanotherium tungurense*, n. sp.), or indet. (? in the tables of appendix 2).

Gur Tung Khara Usu: Type A: AMNH

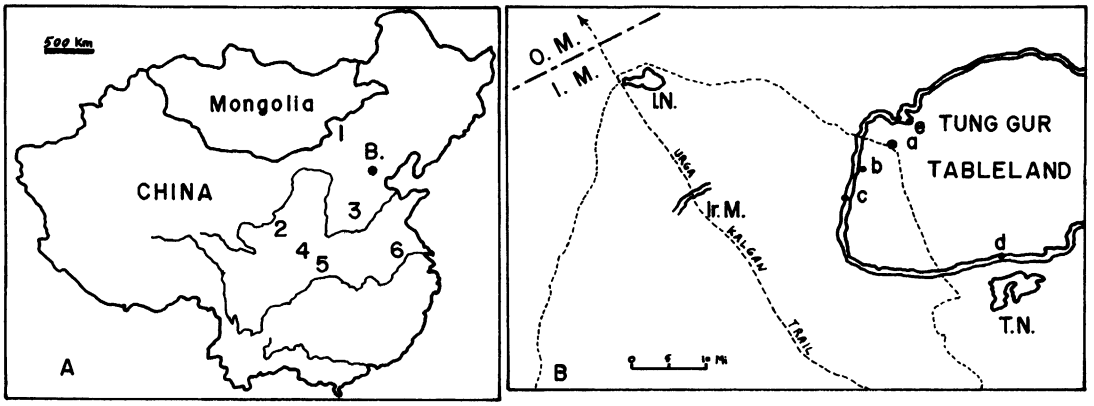

Fig. 1. **A**, Geographical distribution of some Chinese Miocene sites: 1 = Tung-gur, 2 = Tongxin, 3 = Jiulongkou, 4 = Lengshuigou, 5 = Erlanggang, 6 = Lingyanshan, B. = Beijing. Following Qiu (1990). **B**, Detail of Tung-gur area (after Osborn and Granger, 1932): I. M. = Inner Mongolia, Ir.M. = Irdin Manha, I.N. = Iren Nor, T.N. = Tairum Nor, a = Gur Tung Khara Usu, b = Wolf Camp, c = *Platybelodon* Quarry, d = South Camp, e = North Camp.

26520, skull; 26215, skull, mandible, and part of postcranial skeleton of the same individual (17 vertebrae, numerous ribs, r. scapula and l. fragment, r./l. humerus fragments, r./l. ulnae, r./l. radii, r. coxal fragment, r. femur, l. femur fragment, r./l. fibulae, r. patella, r. tibia, and r. McIV); 26523, l. maxillary fragment; 26525, mandible; 26214, 26218, 26524, l. mandibular rami; 26216, r. series p2-m3; 26527, r. juvenile mandibular fragment; 129840, r. humerus; 129837, 129838, r. radii; 129839, l. tibia; 129841, r. tibia; 129890, l. patella; 129925–928, 3 l./1. r. scaphoids; 129942, r. scaphoid; 129835, l. semilunate; 129929, r. pyramidal; 129889, l. pyramidal; 129891, 129892, l. trapezoids; 129915, l. trapezoid; 129893, r. magnum; 129836, l. unciform; 129894, r. unciform; 129930, 129931, 2 l. unciforms; 129933–941, 7 r./2 l. astragali; 129923, 129924, 2 r. calcanei; 129897, 129898, 2 l. calcanei; 129932, r. cuboid (juv.?); 129918, l. McIII; 129899–901, 3 l. McIII; 129921–922, r./l. McIV; 129920, l. MtII; 129902, 129903, 2 r. MtII; 129904, 129919, 2 r. MtIII; 129894, l. cuboid, l. MtIV, and central and lateral phalanges.

Type B: 26217, r. mandibular fragment; 129967, r. pyramidal; 129966, l. navicular.

Indet.: 129989, r. astragalus; 129995, l. McII; 129993, l. MtIII; 129994, r. MtIV.

Tairum Nor Basin: Type A: 26220, skull; 26221, l. mandibular ramus; 26222, mandible fragment; 129831, l. tibia, r. scaphoid, r. semilunate, r. pisiform, r. unciform, r. calcaneum, l. astragalus, l. navicular, l. cuboid, l. mesocuneiform, r. McIII proximal fragment, first central phalanx; 129832, l. navicular.

Wolf Camp Quarry: Type A: 26522 (0.5 mi. N Wolf Camp), skull fragment; 26581a, r. pyramidal; 129833, l. unciform; 129834, r. cuboid; 129909–911, 3 r. astragali; 129907, 129908, 2 l. calcanei; 129914, l. entocuneiform (A?); 129912, l. MtIII; 129913, l. MtII; without catalogue number, central and lateral phalanges.

Type B: 26531, skull; 26519, nasal fragment; 26532, cranial fragment; 26530, maxilar fragment; 129944, r. maxilar; 26577, l. M3; 26542, l. D1-D4; 129943, l. juvenile mandibular fragment; 26528, mandible; 26540, 26541, 26578, 26579, 26580, mandibular fragments; 129945, r. femur; 129974, l. scaphoid; 129975, r. semilunate; 129976, 129977, 2 l. pyramidals; 129978, r. pisiform; 129979, r. magnum; 129980, r. astragalus; 129981, 129982, 2 r. calcanei; 129963, 129964, 2 l. cuboids; 129983, l. navicular; 129984, l. ectocuneiform; 129965, first central phalanx; 129985, central and lateral phalanges.

Indet.: 129990, l. scaphoid; 129996, l. ectocuneiform; 129988, r. navicular.

***Platybelodon* Quarry**: Type B: 26521 (5

mi. SW), juvenile skull and mandible; 26529, 26533, 26537, incomplete juvenile mandibles; 26526, r. mandible; 129950, cervical and dorsal vertebrae; 129948, lumbar vertebra; 129947, l. scapula; 129946, r. tibia and fibula; 129960, r. pyramidal; 129961, l. pisiform; 129949, l. cuboid; 129953–55, 2 r./1 l. McII; 129956, l. juvenile McII; 129951–52, r./l. McIII; 129957, r. McIV; 129959, l. juvenile McIV; 129962, central phalanx; without catalogue number, 2 lateral phalanges.

Without specified locality (only Chahar Province): Type A: 129842, nasal fragment; 129843, 129844, radius fragments; 129845, r. semilunate; 129846, r. pyramidal; 129848–850, 3 r. calcanei; 129851–853, 1 l./2 r. astragali; 129847, l. cuboid; 129855–857, 1 r./2 l. McIII; without catalogue number, central and lateral phalanges (different type).

Type B: 129969, 129970, 2 l. pyramidals; 129972, 129973, 2 r. unciforms; 129971, l. trapezoid; 129958, l. McIV.

Indet.: 129991, l. scaphoid fragment; 129987, l. calcaneum; 129986, r. astragalus; 129992, r. ectocuneiform.

METHODS

The methodology of this study follows previous global works on rhinos (Guérin, 1980; Cerdeño, 1989), emphasizing characters considered in the recent cladistic analysis of the family Rhinocerotidae (Cerdeño, 1995). Based on this previous work, the phylogenetic relationships of the identified species have been established through cladistic methodology, using Hennig86, version 1.5 (Farris, 1988). The primitive perissodactyl *Hyrachyus* has been used as the outgroup. Most of the 47 rhinocerotid taxa considered for the analysis are at the generic level; only those closer to the studied material have been treated at the specific level. The characters and character states follow those established for the analysis of the family (Cerdeño, 1995: table 2). Only character 60 has been modified: it is now considered binary (eliminating character state 2). Consequently, the characters left unordered have been reduced to five (1, 2, 11, 47, and 50).

Common abbreviations used in the text and tables are provided in appendix 1.

SYSTEMATICS

FAMILY RHINOCEROTIDAE OWEN, 1845

SUBFAMILY ACERATHERIINAE DOLLO, 1885

Genus *Acerorhinus* Kretzoi, 1942

Hoploaceratherium Ginsburg and Heissig, 1989. NEW SYNONYMY.

Type Species: *Acerorhinus zernowi* (Borissiak, 1914).

Acerorhinus zernowi (Borissiak, 1914)

DESCRIPTION

This species corresponds to type A cited in the text and tables.

1. SKULL (appendix 2, table 1; figs. 2, 3A): Large size. Dolichocephalic. Sagittal crest present, wider on AMNH 26215 (32.1 mm minimum) than on AMNH 26220 (19 mm) and AMNH 26520 (14 mm). Strong occipital elevation. Nasal bones long, with smooth groove between them; laterally curved, with minimal rugosity on tip. Projecting anteorbital apophysis. Wide supraorbital apophysis. Frontal width at this point lesser on AMNH 26520. Nasal incision reaching P3 level (distal part), or P4 level on AMNH 26520 and 26522. Anterior border of orbit above M1. Infraorbital foramen subdivided by thin septum (complete on AMNH 26220, incomplete on AMNH 26520, apparently absent on AMNH 26215). Occipital face nearly vertical or hardly inclined forward, high and proximally narrow, with expanded lateral crests. On AMNH 26520 occipital face more clearly inclined forward and its lateral edges more markedly concave. Post-glenoid and post-tympanic apophyses separated on AMNH 26215 (closer at left side), in contact on AMNH 26220, and practically fused on AMNH 26520. Post-tympanic apophysis distinguished from much longer paroccipital one.

Premaxillary bones not preserved on any skull.

2. MANDIBLE (appendix 2, table 1; fig. 3B, C, D): Large, with long horizontal ramus slightly extended backward, beyond condyle level; at this point, ramus forms wide and rough margin that curves laterally. Coronoid apophysis pointed and curved backward. Condyle very wide, with strong posterior

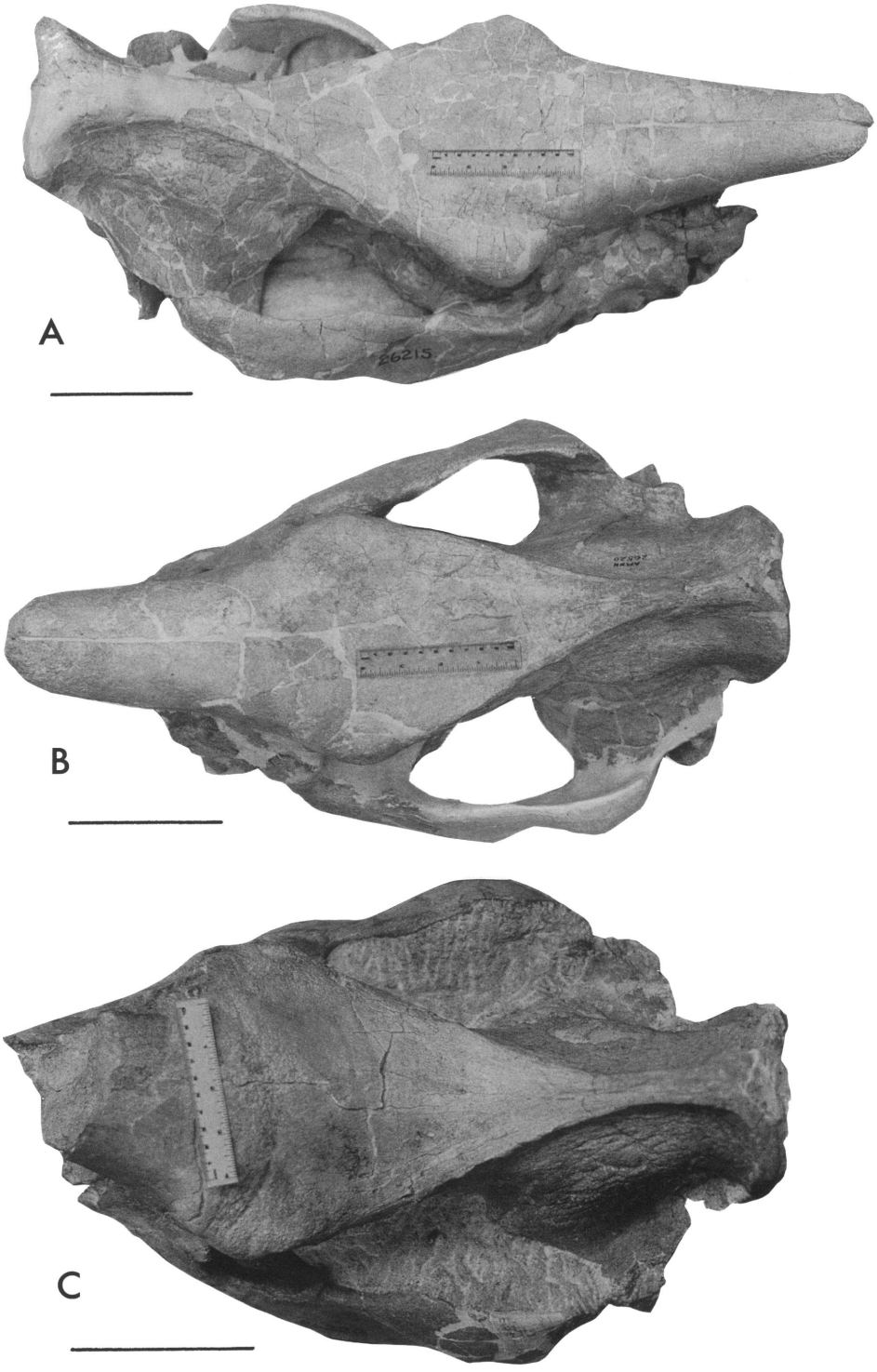

Fig. 2. *Acerorhinus zernowi*. **A**, Skull, AMNH 26215, dorsal view. **B**, Skull, AMNH 26520, dorsal view. **C**, Skull, AMNH 26220, dorsal view. Scale: 10 cm.

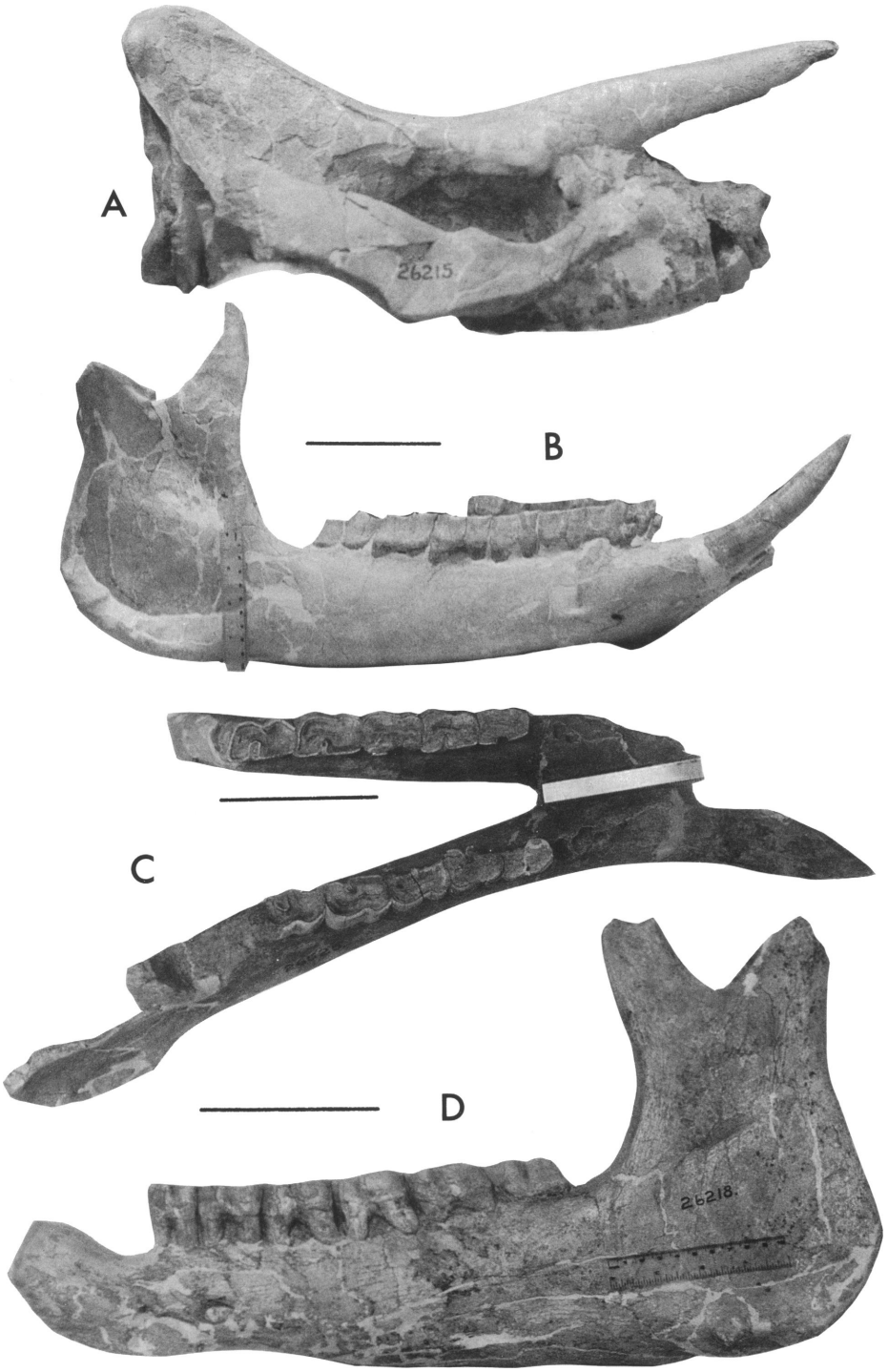

Fig. 3. *Acerorhinus zernowi*. **A**, Skull, AMNH 26215, lateral view. **B**, Mandible, AMNH 26215, lateral view. **C**, Mandible, AMNH 26525, dorsal view. **D**, Mandible, AMNH 26218, lateral view. Scale: 10 cm.

apophysis. Lower profile of horizontal ramus rather straight, with slight elevation of symphysis. Wide symphysis, with flattened labial face and quite concave lingual face, extends back to p3 level. Several mental foramina on labial symphyseal face. Specimen AMNH 26214 shows greater angle between symphysis and horizontal ramus.

3. ANTERIOR DENTITION: No upper incisor is preserved among the studied material from Tung-gur, and it can be assumed that both forms, A and B, lacked I1. However, some mandibular fragments have some of the lower incisors preserved. Type A has i2 as large tusks (fig. 3B) somewhat dorsoventrally flattened and little bent. Specimen AMNH 26222 presents two small i1.

Dimensions of i2 (TD × APD): AMNH 26525, 43.9 × 29.3; AMNH 26215, 36.3 × 26.4.

4. UPPER CHEEK TEETH (appendix 2, table 2; fig. 4A, B): Premolars scarcely represented, all rather worn. Ectoloph has narrow paracone fold and no metacone fold. Protocone limited by slight anterior and posterior grooves on P4. Well-developed crochet, bifurcated on P2-P3 (AMNH 26215); a crista can also be present (P4 of AMNH 26520). All premolars have lingual cingulum, continuous on AMNH 26215 and 26522, and reduced to exit of median valley on AMNH 26520 and 26523. No labial cingulum. Molars have more constricted protocone and larger crochet; their ectoloph slightly convex behind wide paracone fold. Posterior cingulum of M3 strong and high, W-shaped on AMNH 26523. Cement remains present on ectoloph of some teeth (AMNH 26215, 26520).

5. LOWER CHEEK TEETH (appendix 2, table 2; figs. 3B, C, D, 4C): Wide teeth, with marked, but not deep, labial groove on premolars and much shallower groove on molars, particularly the m1-m2, which show a certain swelling on this area similar to that observed in some teleoceratine species (Cerdeño, 1993). Most teeth do not have labial or lingual well-developed cingula, although a labial rugosity is present on several premolars (markedly on the posterior lobe of p2 AMNH 26218), as well as a tubercle on the labial fold of p4 and m2 of AMNH 26218, and both m3s of mandible AMNH 26525. These same m3s show the particularity of having a posterior rounded projection of the metaconid that remains isolated on the right specimen. Mandible AMNH 26214, instead, presents all of its teeth with a labial cingulum, continuous on p2 and m2-m3, and the labial groove is deeper. Series AMNH 26216 (p2-m3) also shows a labial cingulum on the premolars, continuous on p2-p3, and m2 and m3 with a tubercle; these teeth have, instead, a wide and shallow labial groove. This m3 presents in addition a "faux fond" (false bottom) in its anterior valley, a character considered by Guérin (1980: 239) as typical of the genus *Aceratherium* (s.l.).

Mandible AMNH 26215 (fig. 3B) presents two p1, very small with respect to p2, not reaching the occlusal level of the rest of the series. Mandibles AMNH 26222 and 26525 also show one-rooted p1 alveoli. Mandible AMNH 26214 differs from the others in lacking the alveolus of p1. Both this mandible and specimen AMNH 26218 have m3 shorter than m2 (appendix 2, table 2).

6. POSTCRANIAL SKELETON: Most postcranial remains from Tung-gur seem to belong to a single species, type A. The specimens numbered AMNH 26215 belong to one individual (together with skull and mandible AMNH 26215) and the description will focus on them, although only an McIV represents the distal part of the limbs.

Atlas (AMNH 26215; fig. 5A). Large, with wide alae that hardly overlap APD of vertebral corpus. Dorsal tubercle forms median transverse crest. Posteroventral apophysis, rough and narrow, projected in both directions. Anterior articular facets very concave, hardly medially separated. Posterior facets for axis very wide, roughly subrectangular in outline, but with distal border clearly convex. Neural channel pear-shaped in posterior view.

Dimensions (mm): TD max. = 300; TD ant. art. = 129; TD post. art. = 155.9; TD × H axis facet = 68.3 × 51.1; H × TD foramen (post.) = 64.5 × 48.0; APD min. prox. = 56.7; APD dis. (medial) = 66.1; APD between arts. = 124; H max.= 115.8.

Axis (AMNH 26215; fig. 5B). Relatively high. Proximal spinal process broad and short. Atlas facets slightly convex in middle.

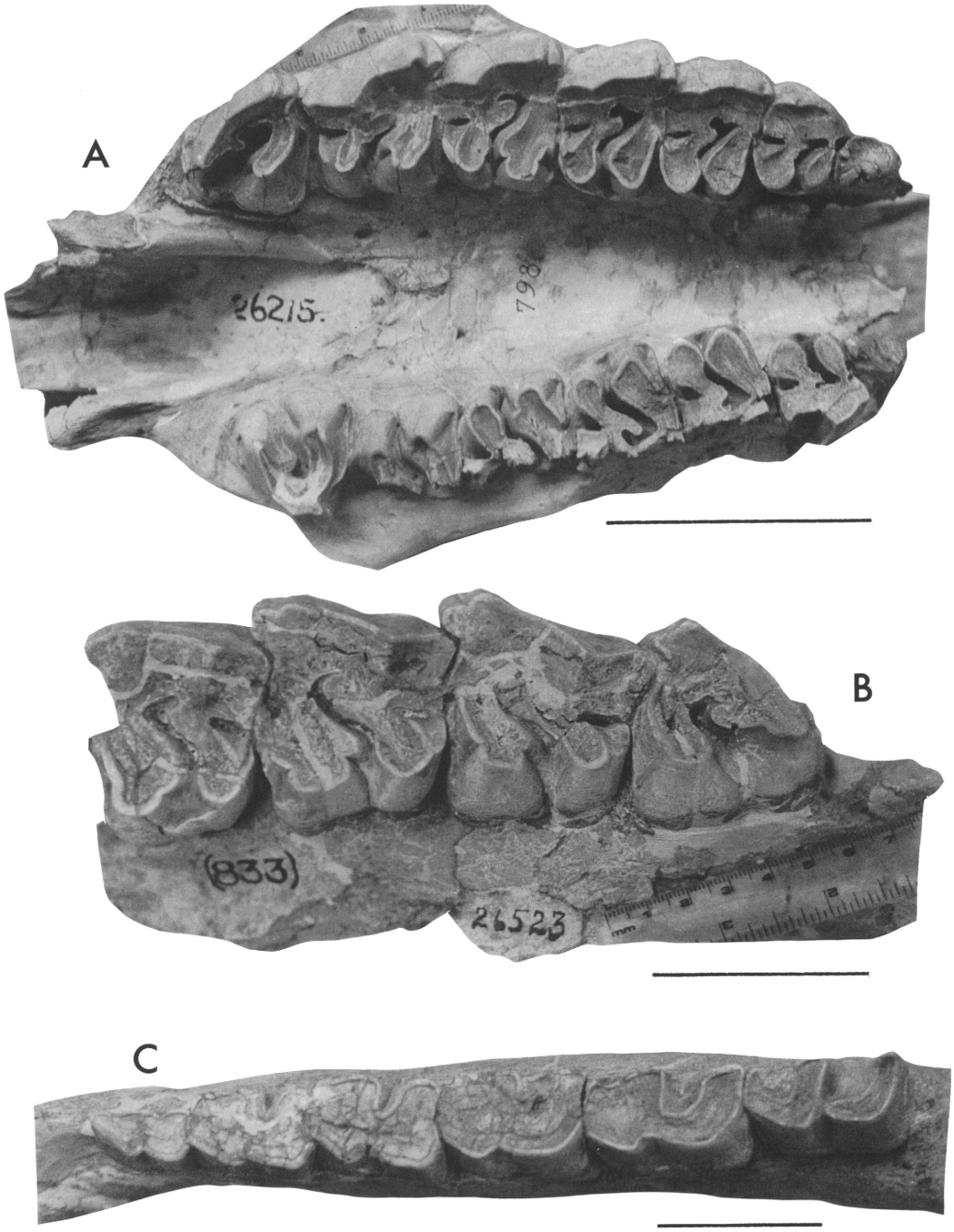

Fig. 4. *Acerorhinus zernowi*. **A**, Skull, AMNH 26215 (detail), occlusal view. **B**, Left P4–M3, AMNH 26523, occlusal view. **C**, Left p2–m3, AMNH 26218 (detail), occlusal view. Scale: A: 10 cm; B, C: 5 cm.

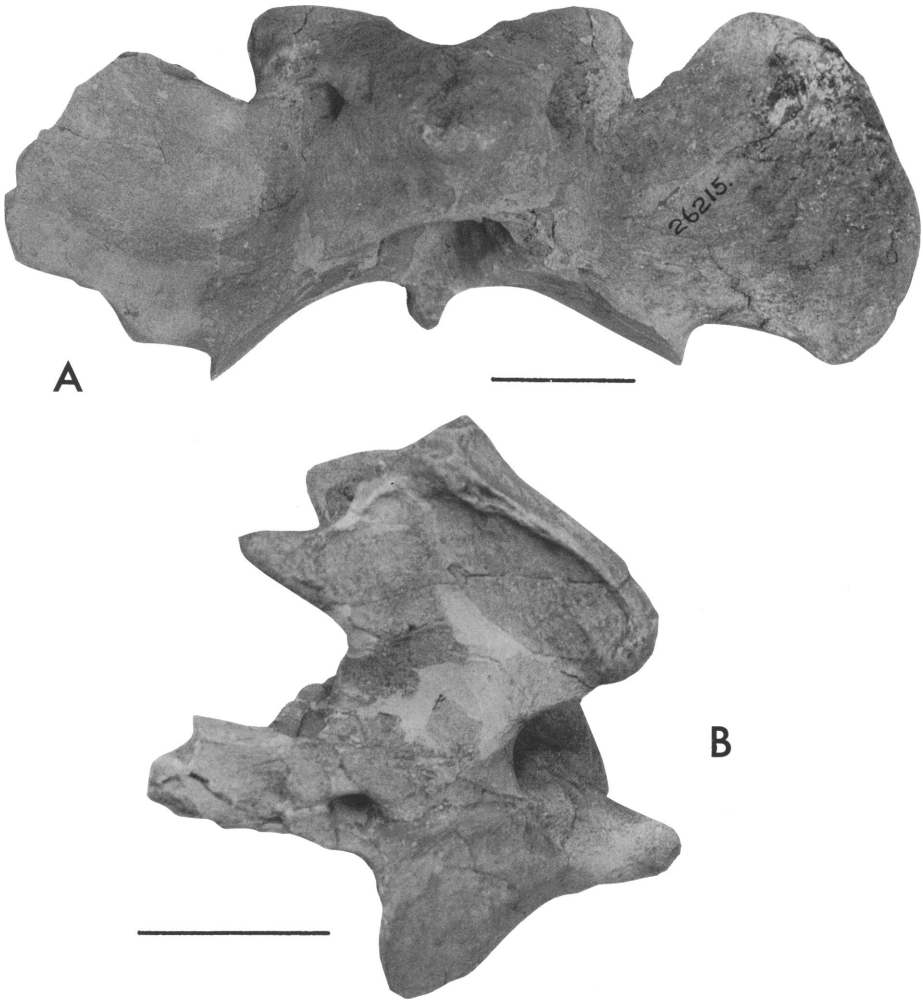

Fig. 5. *Acerorhinus zernowi*. **A**, Atlas, AMNH 26215, proximal view. **B**, Axis AMNH 26215, lateral view. Scale: 5 cm.

Transverse processes very backwardly projected.

Dimensions (mm): TD ant. art. = 155.9; TD transv. proc. = 166.4; TD prox. post. art. = 90.2 ; H max. = 133.5; TD max. prox. crest = 33.1; TD min. prox. crest = 18.8; TD × H ant. art. = 68.3 × 47.2; TD × H post. art. = 65.0 × 63.4; Dens axis = 27.8 × 28.3; APD distal (middle) = 126; APD max. (dens-trans. proc.) = 130; APD prox. crest = 87.7.

Scapula: Specimen AMNH 26215 relatively short in anteroposterior diameter. Scapular spine very large and bent backward, overlaying posterior ridge of scapula. On distal part, supraglenoid tubercle wide, rounded, and rough; separated by narrow, shallow groove from high, narrow, and slightly projected apophysis, placed medially. Articular facet wide, ovoid in outline, and with sharp edge, except at anterolateral zone, where it forms narrow striped border.

Dimensions (mm): Articular diameters = 66.1 × 84.5; APD dis. = 128.1; APD min. = 90.8; APD max. = 221.0; L spine = 113.0.

Humerus (appendix 2, table 3; fig. 6A): As the other long bones, large, not massive, but

with relatively wide epiphyses. Proximal trochanters high and well developed, with wide grooves separating them. Deltoid crest long, its distal tip as curved and projecting rugosity. Lateral epicondyle short and little projected. Small articular trochlea. Deep olecranon fossa.

Radius (appendix 2, table 3; fig. 6B): Shows strong surfaces for muscular insertion; that for biceps large, deep, and slightly medially placed. Proximal facets form rather marked angle between them. Posterior facets for ulna fused. Diaphysis enlarges to wide distal epiphysis.

Ulna (appendix 2, table 3): Robust, with wide and short olecranon. Medially, presents distal wide radius facet.

Coxal: Unique preserved fragment (AMNH 26215) shows only part of ilium and half articular surface. Proximal edge of ilium forms very broad distal tuberosity (91.5 mm). Anterior border between this tuberosity and articulation forms almost right angle.

Femur (appendix 2, table 3): Specimen AMNH 26215 has proximal epiphysis incomplete and third trochanter broken (TD > 103 mm), although it can be deduced that it was quite protruding. Femur rather long, with broad diaphysis and very asymmetric distal trochlea.

Patella (appendix 2, table 4): High and not very broad, with little anteroposterior diameter. Specimen AMNH 129890 differs little from AMNH 26215 in having thicker proximolateral surface and slightly smaller size.

Tibia (appendix 2, table 3): Specimen AMNH 129839 (fig. 6C) has high proximal crest. Anterior tibial groove broad. Tibial tuberosity rounded, slightly separated from proximal area. Distal articulation narrow.

Fibula (appendix 2, table 3): AMNH 26215 specimens have proximal epiphysis with strong tuberosities, little extended over diaphysis. Distal epiphysis has deep and narrow external groove, and articular surface composed of small tibial facet and larger astragalar facet. Diaphysis relatively broad, roughly rectangular in section.

Carpus/Tarsus (appendix 2, tables 5, 6): Several sets of carpal and tarsal bones show the existence of two main morphological types: one of them is somewhat smaller and is correlatable with the skeleton referred to type A, and the other is correlatable with type B. For some bones, a third morphology is observed, as explained later.

Scaphoid (appendix 2, table 5; fig. 6D, E): In type A, scaphoid long, not especially broad, with long proximal articulation whose lateral edge barely exceeds lateral tuberosity. Presents two lateral facets for semilunate and a posterior, almost flat area, laterally directed, better defined as a third facet only on specimen AMNH 129831. The posterior border of scaphoid is little convex and short on AMNH 129831, 129925, and 129926, whereas it is much more convex on AMNH 129927, 129928, and 129942, which present a slightly smaller size (appendix 2, table 5).

Semilunate (appendix 2, table 5; fig. 6F): None of the specimens AMNH 129831, 129835, and 129845 shows a third lateral facet, as expected from the scaphoids. Even specimen AMNH 129831, which seems to belong to the same individual as scaphoid AMNH 129831, lacks such a facet. Proximal facet articulates with radius only. Posterior border of proximal facet extends medially. Distally, magnum facet very long, extended forward. The inferior medial facet is greater on AMNH 129831, and its limit fades into the corpus of the bone. Specimen AMNH 129835 is smaller than the other two (appendix 2, table 5), and it probably corresponds to a juvenile individual.

Pyramidal (appendix 2, table 5; fig. 6G): Out of the ten pyramidals of the sample, AMNH 26581a, 129889, 129929, and 129846 are assigned to type A. They are relatively high and narrow, and so are the medial facets.

Pisiform (appendix 2, table 5): Specimen AMNH 129831 small, with marked neck behind proximal facet. Distal border quite straight, whereas posterior and proximal ones form a great convexity. Lateral face rough; medial face concave. Proximal facet concave, distal one hardly convex; crest between both facets smooth.

Trapezoid (appendix 2, table 5): There are four specimens that differ mainly in size. The three smallest ones are ascribed to the acerathere species.

Magnum (appendix 2, table 5; fig. 6H): Magnum AMNH 129893 long, with well marked incisure behind proximal apophysis;

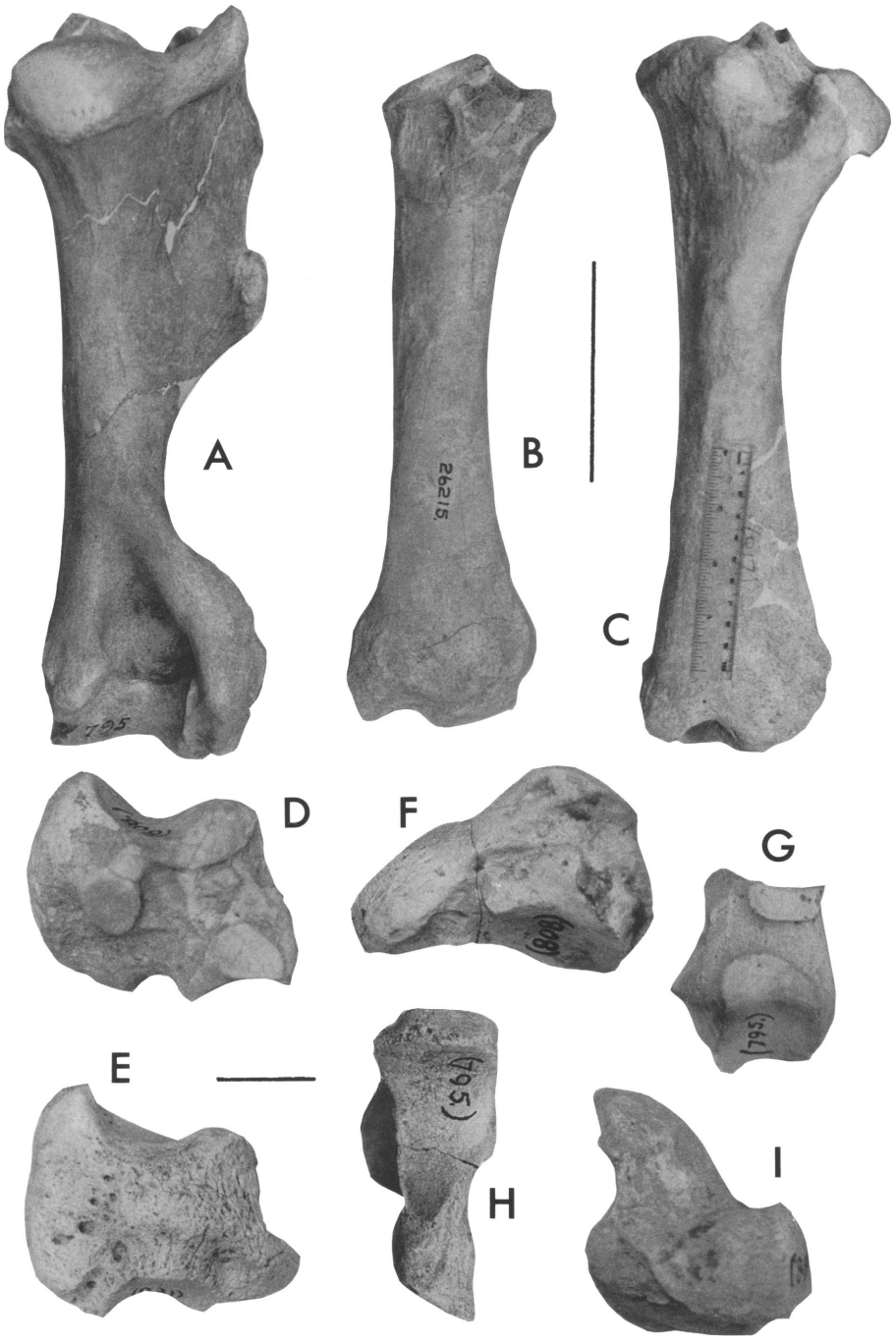

Fig. 6. *Acerorhinus zernowi*. **A**, Right humerus, AMNH 129840, anterior view. **B**, Left radius, AMNH 26215, anterior view. **C**, Left tibia, AMNH 26215, anterior view. **D**, Right scaphoid, AMNH 129831, lateral view. **E**, Left scaphoid, 129925, medial view. **F**, Right semilunate, AMNH 129831, medial view. **G**, Left pyramidal AMNH 129889, medial view. **H**, Right magnum, AMNH 129893, distal view. **I**, Right unciform, AMNH 129831, proximal view. Scale: A–C: 10 cm; D-I: 3 cm.

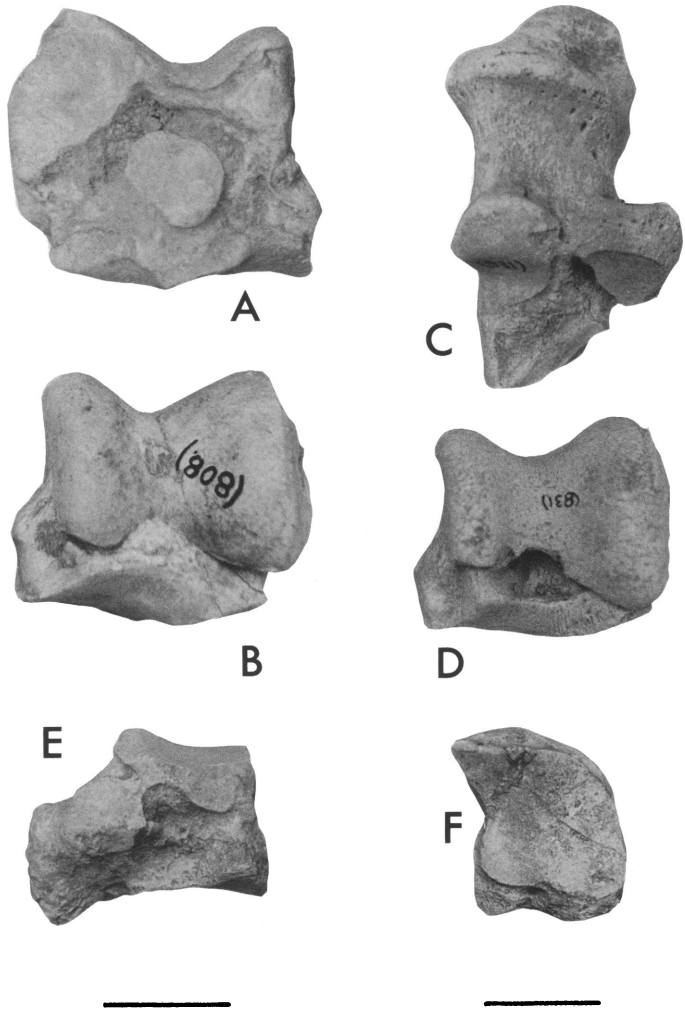

Fig. 7. *Acerorhinus zernowi*. **A**, Left astragalus, AMNH 129831, posterior view. **B**, Same, anterior view. **C**, Right calcaneum, AMNH 129923, anteromedial view. **D**, Left astragalus, AMNH 129935, anterior view. **E**, Left cuboid, AMNH 129831, medial view. **F**, Left navicular, AMNH 129831, proximal view. Scale: 3 cm.

anterior face relatively narrow, with projecting proximomedial apex; distal facet very long, extended over posterior apophysis, with lateral edge rather straight. Proportions not very different from those of the larger type B later described.

Unciform (appendix 2, table 5; fig. 6I). Besides different size, the morphological difference among the unciforms of the sample is in the posterolateral projection of the proximal facet, present on AMNH 129831, 129930, and 129931, where it reaches the lateral border; AMNH 129836 and 129833 present a certain projection, but the limit of the facet fades into the bone before reaching the border. Another unciform (AMNH 129894) is incomplete in this area; its size is closer to specimens considered to be type A.

Astragalus (appendix 2, table 6; fig. 7A, B, D): The astragalus is by far the best represented bone within the sample from Tunggur (21 specimens, some badly preserved). Most of the astragali, considered to be type A, are short and thick (APD), with relatively

deep trochlea, slightly oblique, whose lateral lip extends over distal articulation (and clearly surpasses it in one specimen); groove between trochlea and distal facets generally short and deep, although it can also be shallower; medial tubercle generally little projected and mainly developed in anteroposterior direction; sometimes it reaches distal articular border. On posterior face, facet 1 rather concave, with long distal extension, triangular in shape, stretching distally and laterally. Facet 2 rounded, detached from rest of face; usually isolated by surrounding deep groove, and in two cases united to facet 3 (in these cases facet 2 is greater).

Calcaneum (appendix 2, table 6; fig. 7C): Type A comprises short and robust bones. Tuber broad and high, with smooth unevenness; rather long, but does not surpass anteriorly the beak level. Sustentaculum varies in length, pointed and at right angle with corpus. Tibial facet present in some specimens. Astragalar facets separated, except in one specimen in which facet 2 is wider and is fused to facet 3 through a narrow area.

Cuboid (appendix 2, table 6; fig. 7D): Specimen AMNH 129831 corresponds to the same individual as astragalus and calcaneum AMNH 129831. This and some other specimens of the same type present the anterior face higher than broad. Two proximal facets little displaced relative to each other (calcaneum facet more markedly forward on AMNH 129831). Medially, posterior area of navicular facet displaced backward, showing marked concavity and making right angle with posterior facet for ectocuneiform. Specimen AMNH 129831 differs from others of this type in the navicular facet, which is nearly isolated from the anterior part and is convex instead of concave; this bone also shows a higher lateral extension of the calcaneum facet. Distal facet for MtIV presents smooth medial entrant. All specimens present strong, distally pointed, posterior apophysis.

Specimen AMNH 129894 (fig. 8C) has slightly greater size and stronger proportions. Its anterior face is roughly squared, the proximal facets hardly present the mentioned displacement, and the distal facet does not present any medial entrant. The medial facets are, however, of the same type. It corresponds to the same individual as the McIV described below as type A morphology. Differences can be ascribed to a particularly strong individual.

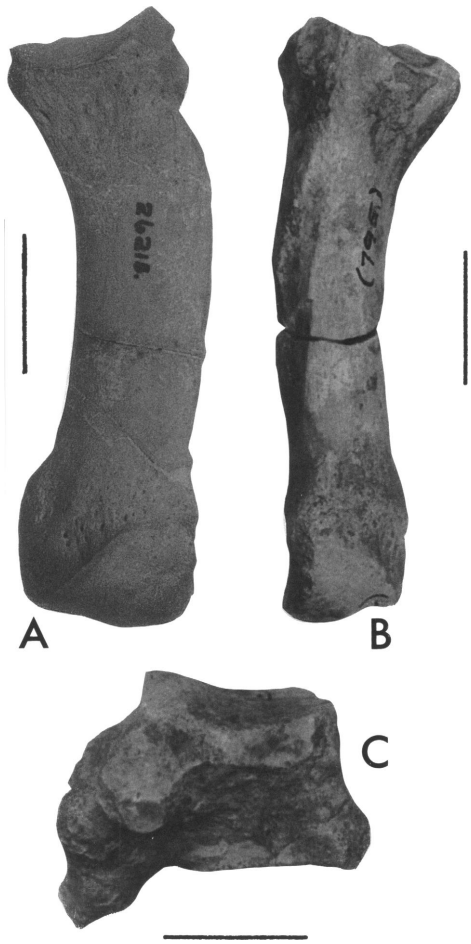

Fig. 8. *Acerorhinus zernowi*. **A**, Right McIV, AMNH 26215, anterior view. **B**, Left MtIV, AMNH 129894, anterior view. **C**, Left cuboid, AMNH 129894, medial view. Scale: 3 cm.

Navicular (appendix 2, table 6; fig. 7F): Two left specimens AMNH 129831 show the same morphology, and one of them belongs to the same individual as the described cuboid AMNH 129831. In proximal view, facet points anterolaterally, its profile more rounded on one of the specimens. Union between anterior and posterior parts of cuboid articulation very narrow (as it was on cuboid AMNH 129831); anterior part triangular in shape and nearly reaches distal border; pos-

terior part concave and extended backward. Distally, entocuneiform facet forms marked angle with mesocuneiform facet.

Mesocuneiform (appendix 2, table 6): The only specimen within the sample corresponds to individual AMNH 129831. Rectangular-outlined, lateral facet missing. Proximal facet concavoconvex in anteroposterior direction.

Entocuneiform (appendix 2, table 6): There is only one specimen (AMNH 129914). It is small, with relatively short distal apophysis that projects posteriorly. Lateral facets widely separated; that for MtII high and narrow.

Metacarpals (appendix 2, table 7): Skeleton AMNH 26215 (type A) includes only *McIV* (fig. 8A). It is a rather slender bone, with broad epiphyses; the proximal one is quite inclined with respect to the major axis and implies a great divergence of the lateral metapodial from the central one. The proximal facet is trapezoidal-outlined, posteriorly and medially elevated; this one and the anterior medial facet form a crest at an open angle. The posterior medial facet is wide, round, and displaced backward, marking the posterior end of the bone; it is in contact with the proximal facet. The McV facet is very reduced.

The same pattern is shared by the other two McIV specimens. AMNH 129922 is shorter (appendix 2, table 7) and more robust.

There is a difference in size among the *McIII* ascribed to type A (appendix 2, table 7; fig. 9A, B). They have a high proximal crest, and the magnum facet stretches markedly backward. The size and form of the lateral and medial facets vary, and the posterior lateral one can be in contact with or separated from the proximal facet, but there is no correspondence between these differences and the different overall sizes of the bones. The distal articulation has a very convex proximal border. This type of McIII corresponds to magnum AMNH 129893 and McIV AMNH 26215, 129921, and 129922.

There is no McII belonging to the acerathere species.

Metatarsals (appendix 2, table 7). The *MtII* show certain differences in robustness and minor morphological differences in the junction or separation of the lateral facets with respect to the proximal articulation. Both lateral facets are separated on AMNH 129903 (fig. 9D), whereas the posterior one is united on AMNH 129902 and on juvenile

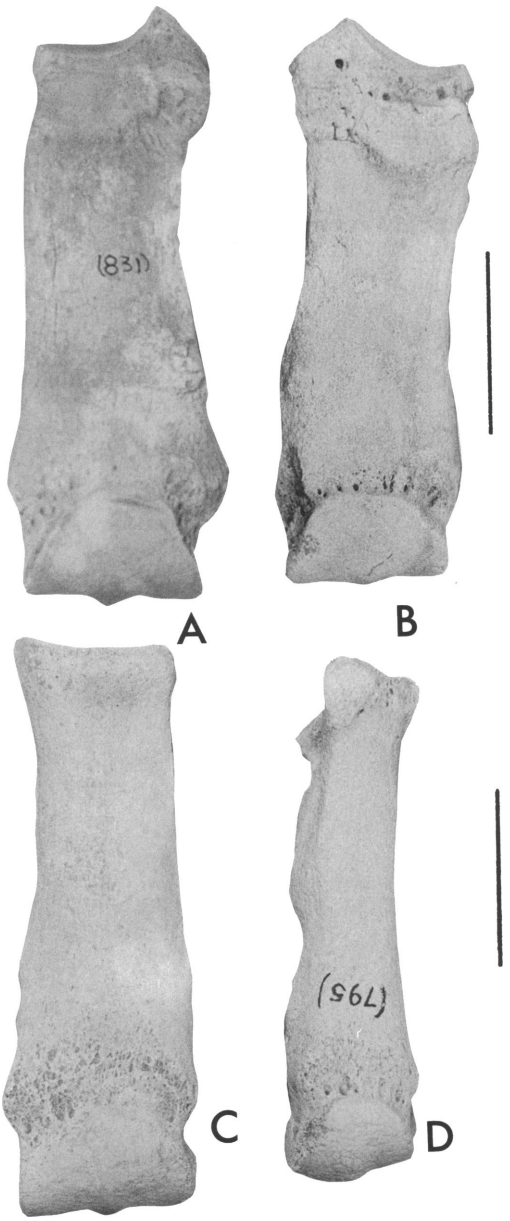

Fig. 9. *Acerorhinus zernowi*. **A**, Left McIII, AMNH 129918, anterior view. **B**, Right McIII, AMNH 129855, anterior view. **C**, Right MtIII, AMNH 129904, anterior view. **D**, Right MtII, AMNH 129903, anterior view. Scale: 5 cm.

AMNH 129920. It is the anterior facet that is united on the stronger specimen, AMNH 129913. The strength of this specimen seems to be an individual particularity, because there are not other major differences. The lateral facets of AMNH 129913 are badly preserved. A high and narrow entocuneiform facet is present on each specimen.

The *MtIII* are not very well preserved. Two specimens (AMNH 129904 and 129912) have a flattened diaphysis that enlarges distally (fig. 9C); on the posterior face, they present a marked supraarticular concavity. The lateral MtIV facets are small and rounded; the proximal facet is slightly transversely concave and presents well-marked lateral and medial entrants.

One *MtIV* (AMNH 129894; appendix 2, table 7; fig. 8B) is a rather strong bone, with marked longitudinal curvature. The proximal epiphysis is roughly quadrangular, with a strong lateroposterior tuberosity; the articular surface is triangular-outlined, longer than broad, with a marked lateral convexity. The medial facets are more or less rounded, with similar overall size. This MtIV seems to belong to the same individual as cuboid AMNH 129894.

Phalanges: As for the other postcranial remains, at least two different types of phalanges are observed, showing different sizes and proportions. Only the best preserved specimens have been measured (appendix 2, table 8). The proportionally shorter first central phalanges, especially AMNH 129905, are tentatively ascribed to type A, as well as the first and second lateral phalanges AMNH 129894.

Discussion

The differences displayed by some specimens of type A do not seem to be sufficient to warrant considering them as separate species. Instead, they seem to correspond to individual or sexual variation. The described characteristics of type A place it within the subfamily Aceratheriinae.

Compared with *Aceratherium depereti* from the Turgai region (Borissiak, 1927), type A from Tung-gur is clearly similar in skull morphology. They share a very concave dorsal profile, which is especially marked in specimen AMNH 26215 (fig. 3A). The sagittal crest seems to be narrower in *A. depereti*, being closer to the condition in skull AMNH 26520. Nasal length is greater in *A. depereti*, although the narrowing of the nasals seems to be less abrupt on the Tung-gur skulls. The post-glenoid and post-tympanic apophyses are close but separated, as in AMNH 26215. The development of the zygomatic arch of *A. depereti* is also quite comparable to this latter specimen (higher and stronger on AMNH 26220). The distance between the nasal incision and the orbit is a little shorter in *A. depereti*, closer to AMNH 26520 than to AMNH 26215. The mandibular characteristics are very similar in both forms. The upper teeth are also equal, while the lower ones of *A. depereti* are a closer match to mandible AMNH 26214. As is the case in the latter, in *A. depereti* the p1 is lacking, and there are well-developed labial and lingual cingula on the premolars. The total length of the upper series varies in *A. depereti* from 225 to 260 mm, and is 261 mm in AMNH 26215. The lower series reaches 250 mm in the former species, and varies from 230 mm in AMNH 26215 and AMNH 26214 to 240.5 mm in AMNH 26218. Craniomandibular features are thus rather close between both populations, but the long and slender limb bones (especially the metapodials) of *A. depereti* (Borissiak, 1927) differ from Tung-gur type A.

Ginsburg and Heissig (1989) suggested that *A. depereti* (including the skulls at the AMNH) could belong to the genus *Hoploaceratherium*. In fact, specimens of Tung-gur type A show many similarities to the type species *H. tetradactylum* (personal observation of the type material from Sansan, France). *H. tetradactylum* is supposed to have had a faint horn boss (Ginsburg and Heissig, op. cit.), although its hornless condition is also supported by other authors (Guérin, 1980). In my opinion, the minimal rugosity on the tip of the nasals is not enough to support any horn. It is hardly more developed than some rugosities that can occur on the supraorbital apophyses of different species. Such nasal rugosity is also present on Tung-gur skulls AMNH 26215 and 26522, and is even less developed in AMNH 26520. Despite the distorted condition of the skulls

of *H. tetradactylum*, their occipital elevation seems to be less than that of the Tung-gur specimens. The mandibular features are coincident in the symphyseal shape, the strong concavity of its lingual face, and the slight elevation with respect to the horizontal ramus. The general sizes of the skulls and mandibles are rather close. The main differences lie in the relatively shorter and wider occipital face of *H. tetradactylum* and in its longer nasals (Guérin, 1980; personal data). The mandibular horizontal ramus is relatively higher in Tung-gur specimens. Type A and *H. tetradactylum* are similar in dentition. The cingulum variation described for the Tung-gur lower teeth is also observed among the French material, where the labial cingulum is usually well developed on premolars, while the lingual cingulum is mainly developed on the anterior lobe. The tooth size of *H. tetradactylum* (personal data) shows a total identity with Tung-gur type A for the upper premolars; the molars are slightly larger (in mean) in type A, although a clear overlap occurs. There is no difference among the lower teeth. The metapodials are slightly stronger in the Tung-gur form: for a similar general size they are relatively shorter. They approach to a certain extent the proportions of the smaller *Alicornops simorrense*. The gracility values of the Tung-gur metapodials (appendix 2, table 7) fall within the range of this species (Cerdeño, 1989: 160), but are closer to the minimum, even below it in the case of the MtIII. Therefore, the degree of slenderness of the acerathere from Tung-gur is intermediate between *H. tetradactylum* and *A. simorrense* (gracility ranges of these two species overlap). The relation (McIII × 100/humerus) reveals a higher value for Tung-gur (42.04, using the mean length of the McIII) than for the latter species (38.0 and 41.6; Cerdeño, 1989), reflecting a relatively longer McIII in the Tung-gur form. *A. simorrense* differs from type A, besides its smaller size, in having longer nasals (incision above P4), more marked symphyseal angle, i2 with a twisted crown and more rounded cross section, and stronger postcranial bones, especially the carpus, tarsus, and metapodials.

One of the curatorial notes mentioned at the beginning of this paper suggested the correspondence of the type A material with North American *Aphelops*. However, this genus (personal observation of the type species *A. megalodus*, AMNH 8292) has shorter and narrower nasals that are slightly inclined downward, less occipital elevation, occipital face inclined forward, relatively narrower and more upraised mandibular symphysis, more convex horizontal ramus, less developed crochet on the upper teeth, and postcranial bones clearly shortened.

Tung-gur type A also presents similarities with some Chinese "diceratheres." These forms were later included within the subgenus/genus *Acerorhinus* (Heissig, 1975; Qiu et al., 1988a). They share the saddle-shaped skull profile with high occiput slightly inclined forward, retracted nasal notch, tapering nasal bones, and absence of I1, characters considered by Qiu et al. (1988a: 498) to be diagnostic of the genus. However, type A lacks other mentioned characteristic features such as the multiplicity of the infraorbital foramina (variable character in the type A skulls; see Description), the ventrally concave symphysis, and the vertical i2 that agree with *Chilotherium* (Qiu et al., 1988a). On the other hand, some outstanding differences among the species included within *Acerorhinus* (Qiu et al., 1988a) are observed. For instance, comparing the skulls of *A. paleosinense* (Ringström, 1924) or "*Aceratherium incisivum*" (Pavlow, 1914) with *A. tsaidamense* (Bohlin, 1937), they greatly differ in the skull dorsal profile, the nasal development, the number of infraorbital foramina (multiple on *A. paleosinense*), and the shape of the symphysis.

Kretzoi (1942) based the genus *Acerorhinus* on the species *Aceratherium zernowi* from Sebastopol (Borissiak, 1914, 1915). This species is coincident with type A in the general shape of the skull and mandible. The presence of a groove between the nasal bones and the breadth of the sagittal crest vary among the specimens (Borissiak, 1915). The infraorbital foramen seems to be double, similar to that of skull AMNH 26220, although this one presents a weaker septum. The upper premolars can present a smooth crista, which disappears with wear, and the crochet is bifurcated on some teeth, such as AMNH 26215.

In terms of general skull shape, *A. tsaidamense* is closer to *A. zernowi* than it is *A. paleosinense*. However, *A. tsaidamense* has a deeper nasal notch (above the anterior part of M1) than *A. zernowi*, and the symphysis is more upraised and is narrowed behind the i2 (itself of small size) on one of the specimens figured by Bohlin (1937: pl. VII). Instead, the symphyseal characters of *A. paleosinense* are close to those of *A. zernowi*, and also to type A from Tung-gur, but the i2 of *A. paleosinense* seems to be more rounded in crown cross section, the skull profile is rather straight, and the occipital crest is relatively wide. All of these features are close to *Chilotherium* (Ringström, 1924) and are also shared by "*A. incisivum*" from Tchobroutchi (Russia; Pavlow, 1914). Therefore, I propose to remove both species, *A. paleosinense* and "*A. incisivum*," from *Acerorhinus*, although a careful, direct study of all this material is needed to establish accurate affinities. The phylogenetic analysis (see below) supports the closer relation of *A. paleosinense* to *Chilotherium* than to *A. zernowi* (fig. 18).

Overall size is similar in all these *Acerorhinus* and type A. The upper teeth are slightly larger in *Acerorhinus*, more markedly in the premolars (P2-P4) than in the molars.

The postcranial bones of type A can be compared with *A. tsaidamense* (Bohlin, 1937), verifying a general smaller size for the latter. Some morphological differences are also observed. The atlas of *A. tsaidamense* has more individualized alae, which are more elongated anteroposteriorly, with their posterior edge surpassing the axis articulation level; the posterior edge reaches the articular level on the Tung-gur specimen (fig. 5A). The humerus shows a wider and higher distal epiphysis. The magnum has a relatively longer posterior apophysis, and the distal articular surface is less extended backward. The calcaneum is shorter. The proximal facet of the McIV is relatively shorter (in APD).

A few data on the postcranial remains of *A. zernowi*, and the figured humerus (Borissiak, 1914: pl. VI), reveal a general similarity with type A.

This discussion makes evident that total identity cannot be established between Tung-gur type A and any of the discussed species. The closest affinities appear to be with *Acerorhinus zernowi*, especially in the craniomandibular features, although postcranial characters cannot be fully checked. Type A is also very close to *Aceratherium depereti* in skull characters, but it differs by its heavier postcranial skeleton. The postcranial bones are rather close to *Hoploaceratherium tetradactylum*, but Tung-gur type A differs in slightly greater robustness as well as some cranial features.

On the other hand, the similarity among most of these forms in cranial, mandibular, and dental features is also evident. Consequently, doubts arise as to their separation at the generic level. Are *A. zernowi*, *A. depereti*, and *H. tetradactylum* so different that they should be ranked as different genera? The comparison is limited to a certain degree by the available figures and by the subjectivity of descriptions. The cladistic analysis (see below and fig. 18) provides an unresolved clade for these species.

Considering the generic diagnosis of *Hoploaceratherium* (Ginsburg and Heissig, 1989: 418), I doubt the postulated presence of a horn on the tip of the nasals, as stated above, and the outline of the referred navicular, as previously discussed (Cerdeño, 1992a). Consequently, the diagnostic characters would involve the high skull with narrow occiput, the lack of I1, the narrow symphysis, the supposed lack of i1, and the enlarged, moderately curved i2. These characters are also those of "*Aceratherium*" *zernowi* (Borissiak, 1914, 1915), which probably had small i1 (Borissiak, 1914: pl VII, fig. 2a). Based on the description of this species, Kretzoi (1942) created the genus *Acerorhinus*, whose distinguishing characters were the short and wide skull, pointed short nasals, deep concave frontal profile, nasal incision posteriorly placed, and high and broad occipital face, inclined forward. However, the figures of Borissiak (1915) show narrow skulls, with relatively long nasal bones, and a high and proximally narrowed occipital face.

Therefore, the main differences between these two species rest in the longer nasal and premaxillary bones of *H. tetradactylum*, a slightly greater distance between the nasal incision and the orbit, and its lesser occipital

height. Despite the deformation of the specimens (Guérin, 1980: pls. 3, 4), these differences can be considered only of specific level.

"*Aceratherium*" *depereti* (Borissiak, 1927) has very long nasals, as long as or longer than *H. tetradactylum*, but the occipital elevation and the position of the nasal incision and the orbit are closer to *A. zernowi*. The long nasal bones of "*Aceratherium*" *depereti*, as well as its slender postcranial skeleton, recall those of *Protaceratherium* (= *Plesiaceratherium*). This genus is well known in the lower Miocene of Eurasia (Yan and Heissig, 1986; Cerdeño, 1989, 1992a), closer in age to "*A.*" *depereti*. However, the cladogram obtained (fig. 18) does not support this affinity: *A. depereti* appears to be closer to the *Acerorhinus* species and *H. tetradactylum* than to *Protaceratherium*.

Therefore, I classify Tung-gur type A as *Acerorhinus zernowi*, keeping in mind the similarities with *H. tetradactylum*, especially with respect to the postcranial skeleton, which is poorly known for *Acerorhinus zernowi*. Synonymy between both genera is proposed, *Acerorhinus* having priority over *Hoploaceratherium*.

SUBFAMILY RHINOCEROTINAE OWEN, 1845

SUBTRIBE IRANOTHERIINA KRETZOI, 1943

Genus *Hispanotherium* Crusafont and Villalta, 1947

Huaquingtherium Huang and Yan, 1983. NEW SYNONYMY.

TYPE SPECIES: *Hispanotherium matritense* (Prado, 1864).

Hispanotherium tungurense, new species

HOLOTYPE: AMNH 26521 (827), juvenile skull and mandible. *Platybelodon* Quarry, Tung-gur Formation, Inner Mongolia, China.

PARATYPE: AMNH 26531, adult incomplete skull; AMNH 26530, upper left series P1-M3. Wolf Camp Quarry, Tung-gur Formation. Other remains listed as type B within the "Material and Methods" section (see above).

ETYMOLOGY: After the Tung-gur Formation.

CHRONOSTRATIGRAPHIC AND GEOGRAPHIC DISTRIBUTIONS: Tunggurian mammal age, Middle Miocene, correlated with upper Aragonian, MN 8 biozone of the European mammalian biochronology. So far known from the Tung-gur region, Inner Mongolia, China.

DIAGNOSIS: *Hispanotherium* of larger size than the other species of the genus. Dolichocephalic skull with nasal development close to *H. matritense*, and greater than *H. lintungensis*. Nasal horn boss little expanded laterally, and placed above the end of the nasal incision. Upper incisors probably lacking, and i1–i2 reduced. Premolar series relatively shorter than in *Hispanotherium matritense*. Postcranial skeleton larger than the latter, with comparable metapodial gracility. General cranial aspect similar to *Ninxiatherium longirhinus* but without nasal septum, and less distance between the nasal incision and the orbit.

DESCRIPTION

1. SKULL: The morphology of skulls AMNH 26531 and 26521 (fig. 10), together with nasal fragment AMNH 26510 (fig. 11A) and skull fragment AMNH 26532, clearly differs from that of the acerathere specimens already described. The most complete specimen is juvenile AMNH 26521. Skull very long and narrow; frontal bone long, wider on adult specimen AMNH 26531. Parietal crests widely separated. Occipital crest smoothly elevated and directed backward, surpassing condyle level. Narrow occipital face, with relatively little lateral enlargement. Post-glenoid and post-tympanic apophyses separated (only preserved on juvenile); both long, latter well differentiated from longer paroccipital apophysis. Nasal bones with rather convex horn boss, hardly laterally expanded even on adult individuals. Both skulls and nasal fragment show horn boss developed over end of nasal incision; nasal bones not fused and stretch forward in narrow and short point. Nasal incision above P3; anterior border of orbit above M2 (adult) and laterally projecting. Distance between nasal incision and orbit greater than in type A (appendix 2, table 1: LIOR). Supraorbital apophysis also well developed.

2. MANDIBLE: Although the most complete specimens of type B are juveniles (fig. 11B),

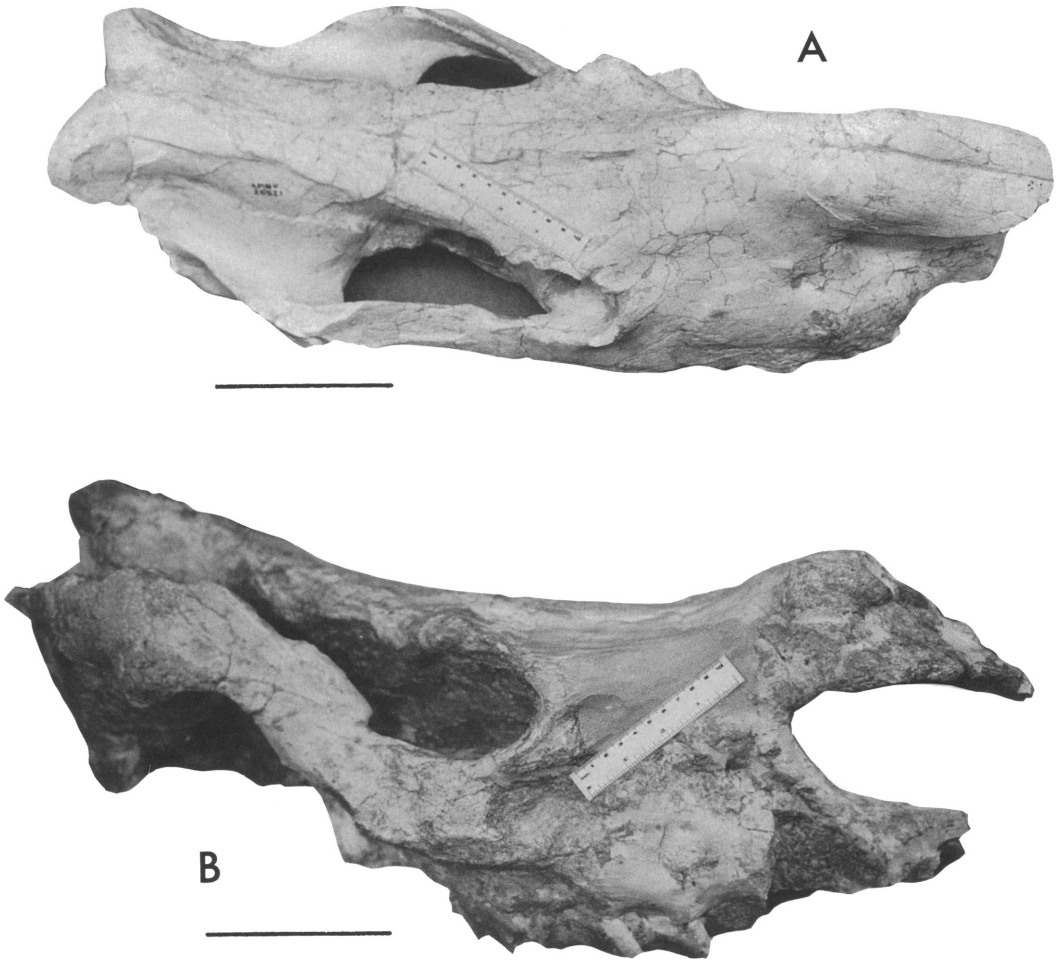

Fig. 10. *Hispanotherium tungurense*, n. sp. **A**, Juvenile skull, AMNH 26521, holotype, dorsolateral view. **B**, Adult skull, AMNH 26531, lateral view. Scale: 10 cm.

the whole sample show a relatively narrow symphysis extended back to the p2 level; the ventral profile on the adults is quite straight. The incomplete ascending ramus appears slightly inclined forward on AMNH 26526, but this may be due to distortion; this ramus is inclined backward on juveniles AMNH 26521 and 26529.

3. ANTERIOR DENTITION: No upper incisor is preserved within the studied sample. Concerning the lower incisors, no mandible has a well-preserved symphysis. Juvenile AMNH 26537 has a di1. Specimen AMNH 26533 also has a di1 root and a small lateral rounded hole that could be the di2 alveolus. Adult AMNH 26526 seems to have alveoli for small i1 and i2. The lower incisors appear to be very reduced.

4. UPPER CHEEK TEETH (appendix 2, table 2; figs. 12, 13B): Type B presents the dental characteristics of the subtribe Iranotheriina (sensu Cerdeño, 1995). Teeth high crowned, with much cement filling in valleys, fossettes, and folds. Ectoloph rather folded, with strong parastyle, paracone and metacone folds developed, and mesostyle. Protocone constricted by anterior and posterior grooves; hypocone somewhat reduced on P3 and P4; metaloph short, very backward directed on M2. Protoloph and metaloph lingually fused

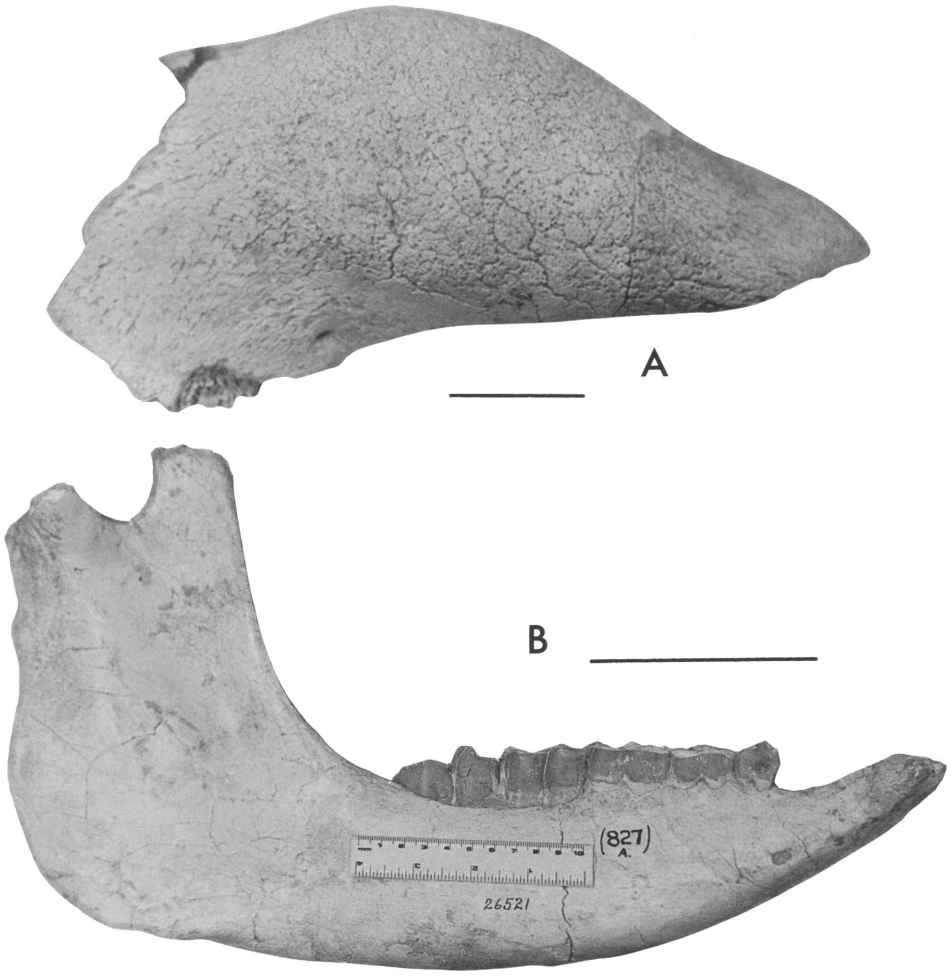

Fig. 11. *Hispanotherium tungurense*, n. sp. **A**, Nasal fragment, AMNH 26519, lateral view. **B**, Juvenile mandible, AMNH 26521, holotype, lateral view. Scale: A: 3 cm; B: 10 cm.

Fig. 12. *Hispanotherium tungurense*, n. sp. Left upper series P2-M2 AMNH 26530 (detail without the erupting M3), occlusal view. Scale: 5 cm.

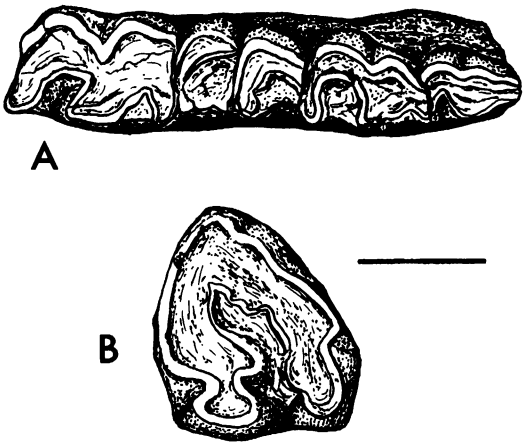

Fig. 13. *Hispanotherium tungurense*, n. sp. **A**, Left p2-m1, AMNH 26577, occlusal view. **B**, Left M3, AMNH 26578, occlusal view. Scale: 3 cm.

on premolars and M1 due to projection of protoloph. Crochet and often a crista developed. On skull AMNH 26531 the teeth are very worn, and the undulation of the ectoloph has almost disappeared. The M2 of this specimen has a labial cingulum, and the M3 shows a strong and narrow posterior cingulum (higher on M3 AMNH 26577); both teeth have a strongly constricted protocone and a great projection of the protoloph. The P4 of skull AMNH 26531 has the protocone more centrally placed on the lingual wall than does the homologous tooth of AMNH 26530. The premolar series is relatively shorter than in type A.

5. LOWER CHEEK TEETH (appendix 2, table 2; figs. 11B, 13A): Present same characteristics of height and cement as upper teeth. The juvenile fragments with m1 already erupted have cement on this molar. The adult specimens lack p1, but a d1 is present in juveniles, one-rooted in AMNH 26529 and two-rooted in AMNH 26521 and 26537. The other permanent teeth have a wide and deep labial groove (depth obscured by cement on AMNH 26528); the anterior valley of the molars is U-shaped, with a long paralophid that marks a strong labial angle, mainly on m2-m3 of AMNH 26526 and 26528. On the premolars, the metaconid is large and extends backward, sometimes clearly delimited by anterior and posterior grooves (AMNH 26541, 26578). This also happens on little-worn molars, as is the case with an m1 wrongly added to a juvenile mandibular fragment of type A (AMNH 129916), where the most proximal part of the metaconid is isolated.

6. POSTCRANIAL SKELETON:

Scapula: Specimen AMNH 129947 relatively much higher (H) and narrower (APD) than type A, with shorter spine that does not reach posterior border. Supraglenoid tubercle more massive and projected. Articular surface broader and shorter, semicircular in shape, with lateral border roughly straight. Anterior border of scapula, even being distorted, laterally curved, in contrast to medially curved AMNH 26215 (type A).

Dimensions (mm): Articular diameters = 72.2 × 79.4; APD dis. = 130.5; APD min. = 105.9; APD max. = (193.5); L spine = 86.1.

Femur (appendix 2, table 3): Incomplete femur AMNH 129945 shorter, with wider diaphysis than type A; third trochanter relatively more distally placed and less projected (TD = 98.8 mm); diaphysis enlarges above it in greater degree than in acerathere specimen AMNH 26215. Medial border forms less marked crest. Distal epiphysis more massive and anterior articulation broader.

Tibia (appendix 2, table 3): Specimen AMNH 129946 large and lacking most of proximal epiphysis; big but slender. Distal epiphysis relatively narrow. Medial facet wider than on AMNH 129839 (type A); lateral facet more flattened.

Fibula (appendix 2, table 3): Fibula AMNH 129946 (united to tibia) long, presenting thinner diaphysis and shallow and wide laterodistal groove.

Scaphoid (appendix 2, table 5): Scaphoid AMNH 129974, although badly preserved, differs from other described specimens of sample in having more flattened articulations.

Semilunate (appendix 2, table 5; fig. 14B, C): Semilunate AMNH 129975 rather massive, with small proximal area of ulnar articulation; medial proximal border forms very projecting point, and superior medial facet very obliquely placed with respect to major axis. Correspondent area for possible third medial facet missing. Laterally, inferior facet very long, almost reaching posterior end of

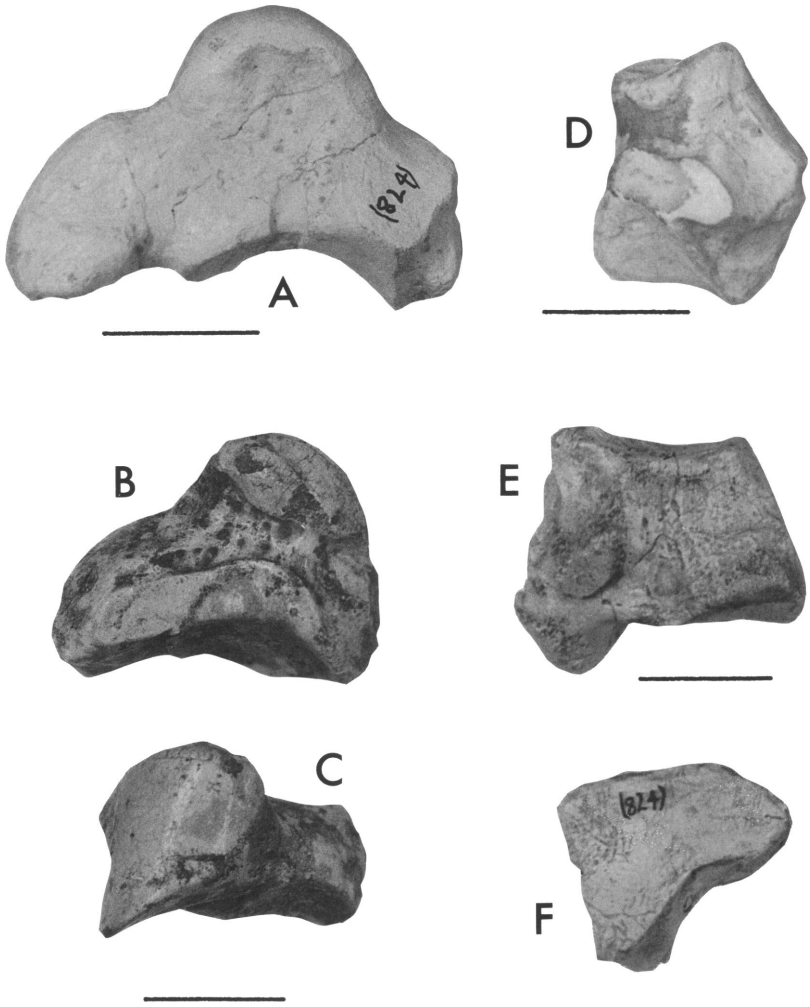

Fig. 14. *Hispanotherium tungurense*, n. sp. **A**, Right magnum, AMNH 129979, lateral view. **B**, Right semilunate, AMNH 129975, lateral view. **C**, Same, proximal view. **D**, Right pyramidal, AMNH 129960, mediolateral view. **E**, Left cuboid, AMNH 129949, medial view. **F**, Left ectocuneiform, AMNH 129984, distal view. Scale: 3 cm.

bone. Distal facet for magnum has short anterior projection.

Pyramidal (appendix 2, table 5; fig. 14D): Compared with type A, broader and shorter, more massive, with wider and less concave facets. Pisiform facet placed at an open angle with proximal facet, and shorter and wider. Distal medial facet for semilunate very extended laterally, although shape of this facet varies among specimens, one (AMNH 129977) even presenting just a little projection. Medial facets short and wide. Specimen AMNH 129967 is very small, probably juvenile; it is badly preserved, but it seems to correspond to type B.

Pisiform (appendix 2, table 5): Specimens AMNH 129978 and 129961 more massive, more regularly outlined, with barely marked neck, than specimen of type A. Facets wider, making acute crest between them. Less lateral rugosities.

Trapezoid (appendix 2, table 5): Only one (AMNH 129971) of the four specimens of the sample presents a greater size, which fits well with the type B McII.

Magnum (appendix 2, table 5; fig. 14A):

Specimen AMNH 129979 much larger than acerathere specimens. Does not present so marked a posterior incisure; proximal facet for scaphoid more flattened, and its union with trapezoid facet better marked by a crest. Main difference concerns distal facet, which in type B is broad and short, without extending backward, and well separated from posterior apophysis.

Unciform (appendix 2, table 5): In contrast to type A, three specimens assigned to type B show the limit of the proximal facet well marked and separated from the lateral border, although a certain extension exists. One of them (AMNH 129854) is very small and could be a juvenile.

Astragalus (appendix 2, table 6; fig. 15C): Type B is represented by specimen AMNH 129980. Broad and short; trochlea little deep, not oblique; distal groove shallow and short. Medial tubercle little developed. On posterior face, facet 1 less concave than type A, with long and narrow extension, marking L-shaped internal border with rest of facet. Facets 2 and 3 fused; facet 2 slightly convex.

Calcaneum (appendix 2, table 6; fig. 15A, B): Two right calcanei, AMNH 129981 and 129982, differ from the others described in several aspects. Besides their larger size, they are high, with a strong tuber that develops in a way different from type A: it draws a convex posterior profile in lateral view, and is more markedly higher medially than laterally in posterior view. Tuber with strong, long unevenness. Astragalus facets wider, especially facet 2, which is nearly in contact with facet 1; facets 2 and 3 separated in both specimens. Tibial facet very large. Small fibular facet could have occurred (eroded area).

Cuboid (appendix 2, table 6; fig. 14E): Specimens AMNH 129963, 129964, and 129949 show a general pattern clearly different from type A. The posterior apophysis is little developed, with slight posterior projection, so these specimens are shorter than those of type A. Anterior face high, irregular due to anterolateral tuberosities. Proximal articulation points backward, especially on AMNH 129963 and 129949. Navicular articulation very reduced at its anterior part, and posterior one hardly extends backward, being more vertical. Ectocuneiform facet faces more distally. Distal facet has rounded an-

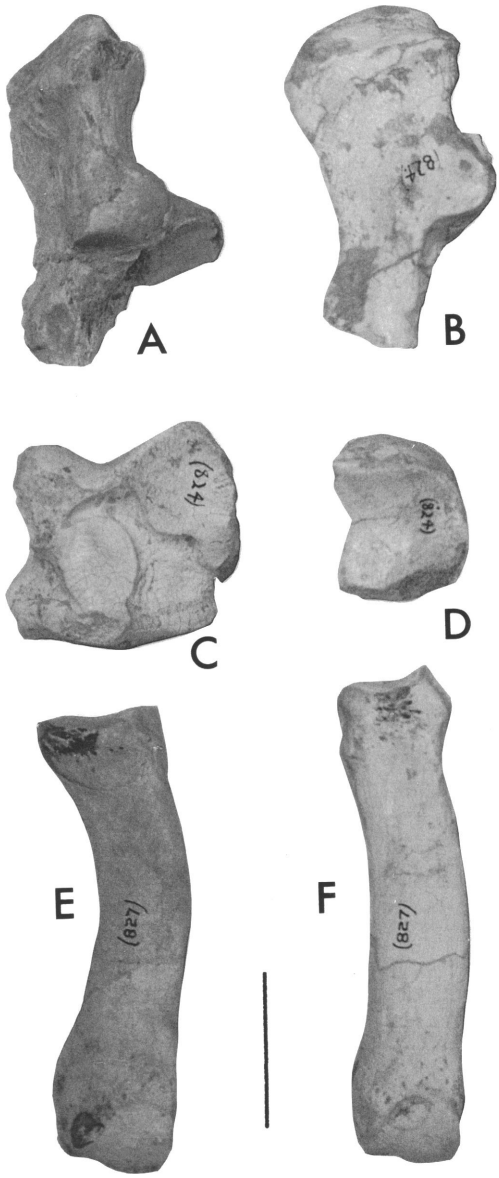

Fig. 15. *Hispanotherium tungurense*, n. sp. **A**, Right calcaneum, AMNH 129981, anterolateral view. **B**, Right calcaneum, AMNH 129982, lateral view. **C**, Right astragalus, AMNH 129980, posterior view. **D**, Left navicular, AMNH 129983, proximal view. **E**, Right McIV, AMNH 129957, anterior view. **F**, Left McII, AMNH 129953, anterior view. Scale: 5 cm.

terolateral outline, does not have medial entrant. The size of these bones is somewhat variable, AMNH 129963 being more massive (appendix 2, table 6).

Navicular (appendix 2, table 6; fig. 15D): The navicular AMNH 129983 differs from the described type A mainly in the lateral facets, because the anterior part is reduced to a narrow strip and the posterior one is high, narrow, and convex. Cuneiform facets do not form marked angle. Little anterolaterally pointed, posteromedial tuberosity short. This specimen corresponds to the same individual as astragalus AMNH 129980.

Specimen AMNH 129966 is markedly larger than all others (appendix 2, table 6), but it does not differ very much from AMNH 129983, except in being more pointed anterolaterally. It is tentatively ascribed to type B.

Ectocuneiform (appendix 2, table 6; fig. 14F): Specimen AMNH 129984 large, broader than long; distal facet rather triangular in shape, with smooth lateral entrant. McII facets semilunate in shape, posterior one oblique to vertical axis, facing slightly distally.

Metacarpals (appendix 2, table 7): The adult specimens of *McII* (AMNH 129953–955; fig. 15F) reflect clear differences in relative individual slenderness. Laterally, they present a flattened, long magnum facet, which forms a smooth angle with the McIII facet; this latter only develops anteriorly. A narrow, rounded tuberosity detaches posteriorly on two of the four specimens. The juvenile shows the same morphology, without this tuberosity. There is a well developed trapezium facet. As the following metapodials, these McII correspond to a slender species with greater general size than the acerathere species.

McIII AMNH 129951 and 129952 are big, long bones (appendix 2, table 7) with a high crest between both proximal facets. The unciform facet and the anterior McIV facet vary in their anteroposterior length between the two specimens. The posterior McIV facet is slightly separated from the posterior end of the proximal articulation, surpassing it backward in one specimen. The medial facet for the McII is wide, mainly anteriorly developed.

McIV AMNH 129957 (fig. 15E) is a much longer bone than type A, with a narrow distal epiphysis. The proximal epiphysis has a more straight lateral profile, because the McV articulation is well developed as a convex border laterally extended. The anterior medial facet is greater and more verticalized than in type A, whereas the posterior one is smaller and well separated from the proximal articular surface. Another McIV (AMNH 129958), which lacks most of the proximal epiphysis, is similar to AMNH 129957, with broader diaphysis and distal epiphysis (appendix 2, table 7).

Metatarsals (appendix 2, table 7): There is no metatarsal of type B. Two small and slender MtIII and MtIV (AMNH 129993, 129994) are considered as Rhinocerotinae indet. (see below), because their size is too small to correspond to the described metacarpals, taking into account that they are adult specimens (epiphyses already fused).

Phalanges: First central phalanges AMNH 129962 and AMNH 129965 fit well with the size of the McIII, although they could perhaps belong to the hind foot, because they do not present a marked central proximal groove necessary for the corresponding keel of the McIII.

First lateral phalanx AMNH 129968 shows a clear morphological difference from AMNH 129894 (type A): the former has the proximal facet with a lateral expansion, separated by a smooth crest from the main articular area, whereas the type A has a rounded articulation. However, this different morphology also seems to correspond to the digit (II or IV) to which the phalanges belong (Iñigo and Cerdeño, in press). The larger size of AMNH 129968 (appendix 2, table 8) matches with type B.

Discussion

The dental features described for type B are easily recognizable as typical of Iranotheriina (sensu Cerdeño, 1995). This subtribe includes the genera *Hispanotherium* Crusafont and Villalta, 1947 (including *Beliajevina* Borissiak, 1938, after Iñigo and Cerdeño, in press) and *Iranotherium* Ringström, 1924. Other taxa formerly considered together with them are *Elasmotherium* Fischer, 1809, and

Ninxiatherium Chen, 1977, the latter being rather close to *Iranotherium* (Cerdeño, 1995). Some other "elasmotherine" forms were described as new genera and/or species, and most of them later synonymized (Heissig, 1972, 1976; Antunes and Ginsburg, 1983; Cerdeño, 1989; Fortelius and Heissig, 1989; Cerdeño, 1995; Iñigo and Cerdeño, in press), in some cases without general agreement—e.g., *Gobitherium mongoliense* (Osborn, 1924); *Begertherium borissiaki* Beliajeva, 1971; *Caementodon oettingenae* Heissig, 1972; *Beliajevina tekkayai* Heissig, 1974; *Hispanotherium lintungensis* Zhai, 1978; and *Tesselodon fangxianensis* Yan, 1979.

One of the best represented species of this group is *Hispanotherium matritense* from Spain (Cerdeño, 1989, 1992a, 1992b; Iñigo and Cerdeño, in press), the Siwaliks, Pakistan (= "*C. oettingenae*"—Heissig, 1972), Mongolia (= "*B. borissiaki*"—Beliajeva, 1971), and Turkey (= "*H. grimmi*"—Heissig, 1976). Unfortunately, none of these areas has provided good cranial remains. Two nasal fragments from Spain and Turkey do not present any horn boss (further comments in Cerdeño, 1995), contrary to the skull of "*B. borissiaki*." Because this species is considered synonymous with *H. matritense*, the existence of possible sexual dimorphism with regard to the presence of a nasal horn is implicit (unless differences between populations are proved by further findings).

The skulls of type B from Tung-gur, especially the juvenile one, resemble that of *Ninxiatherium longirhinus* (Chen, 1977); this is reflected by the collection labels, although the generic name *Iranotherium* is used. They share with that species the general skull shape (long and narrow), the presence of a narrow nasal rugosity, the long distance between the nasal incision and the orbit, and the laterally projecting orbital border. On the other hand, they differ in the presence of a partially ossified nasal septum in *Ninxiatherium*, which is not present in the Tung-gur material. The nasal incision is above P4 in *Ninxiatherium*, so it is deeper than in Tung-gur type B and other iranotherines. The orbit is also very retracted in that taxon, behind the M3 level, even more than in *Iranotherium morgani* (above back M3), although in the latter the nasal incision is, in contrast, less deep (above P3). The free nasal length in *Ninxiatherium* and the skulls of type B is greater than in *I. morgani*. The horn would be relatively more forwardly placed in *Ninxiatherium* than in the Tung-gur specimens.

The type material of "*Begertherium borissiaki*" (Beliajeva, 1971) includes a distorted partial skull that shows a nasal horn boss more retracted than in *Ninxiatherium* and more similar to Tung-gur type B. *Hispanotherium lintungensis* (Zhai, 1978) also has a horn boss apparently less developed and even more backwardly placed. Both species also share with the studied material a great distance between the nasal incision and the orbit. The nasal incision lies above P2 in "*B. borissiaki*" and above the anterior part of P3 in *H. lintungensis*. In *H. lintungensis* the nasal length seems to be relatively shorter than in the others, closer to that in *Iranotherium morgani*, but the nasal is less developed. On the other hand, the skull of "*Beliajevina*" *caucasica* (Borissiak, 1938; Heissig, 1974) also presents a retracted nasal horn boss, near the nasofrontal suture. Its nasal incision is above P3. Iñigo and Cerdeño (in press) consider "*B.*" *caucasica* as a species of the genus *Hispanotherium*.

Hispanotherium lintungensis (Zhai, 1978) comes from a geographical area close to Tung-gur. Huang and Yan (1983) considered it as a distinct genus, *Huaquingtherium*, whose diagnosis was recently revised by Guan (1993), including a second species within the genus, *H. qiui*, from Tongxin. The dental characters of the type material of *H. lintungensis* hardly differ from those of *H. matritense*. Zhai (1978) stated that *H. lintungensis* has less folded enamel than *H. matritense* and that the hypocone has only an anterior groove, whereas the Iberian species has both anterior and posterior grooves. However, the degree of folding of the enamel decreases to a certain extent with wear, as observed also in the Tung-gur material, and the specimen from Lintung is an old individual. The posterior hypocone groove can be very little developed, as on the M1 and M2 of the type material of *H. matritense* (Crusafont and Villalta, 1947).

More significant could be the cranial differences between *H. lintungensis* and "*B.*

borissiaki" with respect to the development of the nasals. The former presents more retracted and shorter nasals, with the end of the incision a little deeper than in the latter (see above), although it coincides with *H. caucasica* in this feature. Considering the incomplete nature of these skulls, I do not agree with the statement about the relatively wider skull of *Huaquingtherium* (Guan, 1993). Therefore, *H. lintungensis* can be maintained within the genus *Hispanotherium*, and *Huaquingtherium* becomes a subjective synonym.

On the other hand, the figures of the species *Huaquingtherium qiui* (Guan, 1993: pl. I) do not seem to correspond to an iranotherine form (at least the lower teeth, which are better reproduced). Qiu (1990: 540) instead referred to an acerathere among the Tongxin fauna. The other "elasmotherine" from Tonxing, *Caementodon tongxinensis* (Guan, 1993: pl. II), is not different from *Hispanotherium matritense*, taking into account the intraspecific variation, and the genus was previously considered a synonym (Antunes and Ginsburg, 1983; Cerdeño, 1989, 1992b; Iñigo, 1993; Iñigo and Cerdeño, in press).

Within "*Begertherium*," Beliajeva (1971) included the species *Gobitherium mongoliense* (Osborn, 1924; Kretzoi, 1943), later considered as a species of the genus *Iranotherium* (Heissig, 1972, 1976). The type material of *G. mongoliense* (skull fragment, AMNH 19185) presents dental characters of subtribe Iranotheriina, but the cranial features are rather different. The nasal bones are very long, narrow and regularly curved anteriorly, without any horn boss, and with lateral apophyses just before the end of the incision (in a pattern similar to primitive rhinos such as *Teletaceras* or *Subhyracodon*). The hornless nasal fragments of *H. matritense* are straight, not curved, very different from *Gobitherium*. In addition, the nasal incision-orbit distance is much shorter than in the other mentioned iranotherines. The orbital border lies above M1, and the incision probably was above P2. The orbital border is not projecting as in iranotherines. A feature that approximates *Gobitherium* to *Iranotherium* is the strong elevation of the zygomatic arch, but even in this case the shape and the angle of the arch are quite different in both forms (see Kretzoi, 1943: fig. 2 for comparative schemes). Therefore, I keep *Gobitherium* apart from *Iranotherium* and also from "*Begertherium*" (= *Hispanotherium*). Although the dental characters of *G. mongoliense* relate it to the iranotherines, as seen in the cladistic analysis (fig. 18), it differs greatly in cranial features. Moreover, because it is so poorly known, its relationships are very uncertain.

Tesselodon fangxianensis (Yan, 1979) is based on just a few dental remains that do not differ fundamentally from those of *Hispanotherium*. Fortelius and Heissig (1989) stated that *Tesselodon* shares with later "elasmotherines" the metaloph of P2 directed backwardly, in contrast to *Hispanotherium*, "*Begertherium*," or "*Beliajevina*." The validity of this character is debatable. For instance, the P2 of *H. matritense* (= *C. oettingenae*) from the Siwaliks (Heissig, 1972: pl. 6) would be comparable to that of *Tesselodon* if it were a little more worn, and the same is true for the specimens from Lisbon figured by Antunes and Ginsburg (1983: pl. XI, figs. 3, 4). "*Tesselodon*" comes from a level equivalent in age to Tung-gur.

The postcranial skeleton of type B from Tung-gur is closely similar to that of *H. matritense*. Some of the features that separate it from type A are also present in that species, such as the presence of the ulnar facet on the semilunate, the long inferior articulation between the semilunate and the pyramidal (less prolonged in *H. matritense*, in which it can vary), the weakly projecting third trochanter of the femur, the characters of the astragalus and the calcaneum, the slender metapodials, and even the phalanx morphology (Cerdeño, 1992b; Iñigo and Cerdeño, in press). Among the metapodials from Tung-gur, the McIV has the proximal facet less triangular in shape than *H. matritense*, although it is not so trapezoidal as in the aceratheres, and the development of its McV facet is equivalent to that of the homologous bones of *H. matritense* from Córcoles (Iñigo, 1993; Iñigo and Cerdeño, in press). Ectocuneiform AMNH 129984 from Tung-gur also differs in being relatively wider. The postcranial bones of *H. caucasica* are equally very similar, although there are some differences in

the trochlea and facets of the astragalus, and in the posterior profile of the calcaneum (Borissiak, 1938), features in which *H. caucasica* also differs from *H. matritense* (further comparison in Cerdeño, 1989, 1995; Iñigo and Cerdeño, in press).

The skull dimensions of the iranotherine from Tung-gur are hardly comparable to other forms, due to their incompleteness or the juvenile condition of the specimens as well as to the lack of published data. Judging from published figures, the distance from the nasal incision to the orbit (LIOR) of *N. longirhinus* is estimated at about 224 mm, greater than the same dimension of the adult skull from Tung-gur (appendix 2, table 1). The nasal width of "*B. borissiaki*" is less (106 mm).

The size of the Tung-gur teeth is similar to that of *H. lintungensis*, although the length is somewhat smaller in this species, probably due to the high degree of wear or perhaps to the points of measurement (at the base of the crown). On the contrary, "*B. borissiaki*" has longer upper premolars; the lower ones seem shorter because they were measured at the base of the crown. Following Chen (1977), the teeth of *Ninxiatherium* are clearly larger than those of the Tung-gur species. Compared with the sample from Córcoles (Spain; Iñigo and Cerdeño, in press), P1 and P2 from Tung-gur are within the range of the Spanish *Hispanotherium*, P3 is slightly longer and wider in Tung-gur, P4 and M1 are wider, and M2 and M3 are clearly greater in both dimensions in the Mongolian sample. Similar differences are seen in lower teeth, in that the molars are relatively greater than the premolars. This is also valid with respect to other *Hispanotherium* populations, whose comparative dimensions can be found in Iñigo and Cerdeño (in press).

The greater size of the Tung-gur material with respect to *Hispanotherium matritense* also extends to the postcranial skeleton. Only some dimensions of the astragalus (TD and H) and the calcaneum (APDT; appendix 2, table 6) are less than the maximal values of *H.* "*grimmi*" and *H. matritense* from Córcoles. The navicular and ectocuneiform AMNH 129983 and 129984 have their APD less than the maximum at Córcoles. The metapodials are larger in Tung-gur, but their gracility index (TD diaphysis × 100/L) is very similar.

In summary, the iranotherine rhinoceros from Tung-gur shows many features that place it close to *Hispanotherium matritense* (s.l.), even with respect to the incompletely known skulls of this species. Cranial characters are also close to *Ninxiatherium*, but this latter differs in the presence of a nasal septum and retraction of the orbit. Based on the present knowledge of the different iranotherines under discussion, the Tung-gur type B specimens can be identified as a new species of the genus *Hispanotherium*, *H. tungurense*, n. sp.

Rhinocerotidae indet.

Some bones from the studied sample from Tung-gur cannot be ascribed to either of the two morphological types identified as *Acerorhinus zernowi* and *Hispanotherium tungurense*, n. sp. Instead, they show clear differences that allow recognition of a third rhinocerotid species.

Description

1. Scaphoid: Two fragmentary specimens (AMNH 129990, 129991) show a greater size than the other Tung-gur taxa (appendix 2, table 5). The most complete, AMNH 129990, has a high and very convex posterior border; there is no third lateral facet, the superolateral facet is wide and fusiform, and the trapezoid facet widely extends laterally. The anterior apophysis is lacking.

2. Astragalus: This third type is represented by a well-preserved specimen (AMNH 129986; fig. 16A, B) and probably also by AMNH 129989. The former specimen is relatively higher and narrower than type A. Deep trochlea higher, not oblique; distal end of medial lip fuses with distal groove. This latter short and shallow. Medial tubercle well delimited and separated from distal border. Calcaneum facets: facet 1 wider and shorter, without distal extension; facet 2 large, high, flat, placed closer to medial face; facet 2 fused to facet 3. Specimen AMNH 129986 also differs from type B (AMNH 129980) in the lack of distal extension of facet 1, and in the medial lip of the deeper trochlea being more acute and narrower.

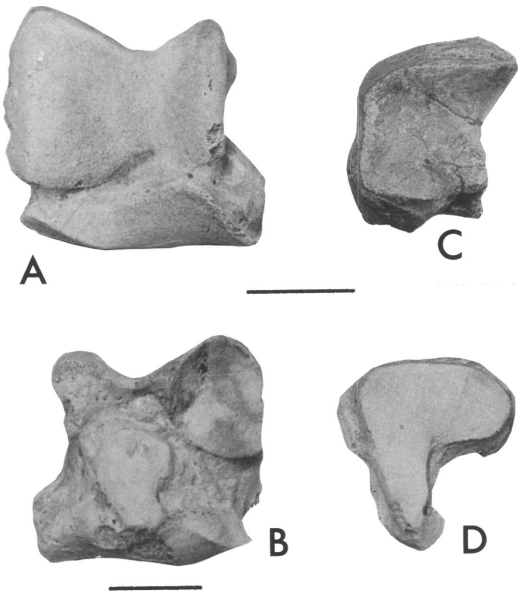

Fig. 16. Rhinocerotidae indet. **A**, Right astragalus, AMNH 129986, anterior view. **B**, Same, posterior view. **C**, Right navicular, AMNH 129988, proximal view. **D**, Right ectocuneiform, AMNH 129992, proximal view. Scale: 3 cm.

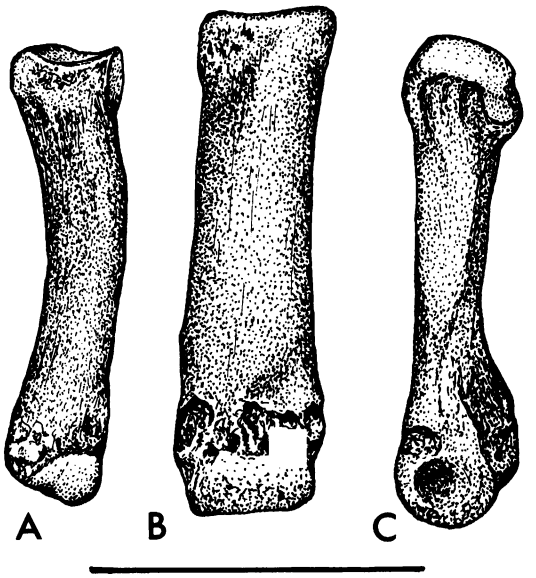

Fig. 17. Rhinocerotidae indet. **A**, Right MtIV, AMNH 129994, anterior view. **B**, Left MtIII, AMNH 129993, anterior view. **C**, Left McII, AMNH 129995, lateral view. Scale: 10 cm.

Specimen AMNH 129989 (eroded) is a large bone that shows a mixture of the features described for each type. It is high and has a deep trochlea, like the third type, but it differs from it mainly in having facet 1 with distal extension and wider proportions. The lateral lip of the trochlea overpasses the distal articular level, as in *A. zernowi*.

3. CALCANEUM: The third type is represented by one specimen (AMNH 129987), which is more slender and higher and has shorter APD than *A. zernowi*. Tuber shorter in APD, higher, with stronger unevenness. Sustentaculum not very long, placed at right angle. Tibial facet greater, semilunate in shape. Astragalus facets separated. Tuberosities for muscular insertion less developed, especially on tuber and neck. Compared with *H. tungurense*, the specimen is smaller, with straighter posterior and lateral profiles, and stronger unevenness of the tuber.

4. NAVICULAR: Specimen AMNH 129988 (fig. 16C) is larger than the two taxa already described, longer than broad, and very high. Proximal facet narrow, with its medial border nearly straight. Laterally, anterior part of cuboid articulation little developed, posterior part high and narrow and quite flat. Distal entocuneiform facet forms greater angle with mesocuneiform facet than in *H. tungurense*. This specimen matches well with the third type of astragalus described above.

5. ECTOCUNEIFORM: The large specimen AMNH 129992 (fig. 16D) is longer than broad and very high. Proximal facet extends backward, with narrow union to rounded, posterior cuboid facet. Posterior MtII facet not so oblique, and almost circular.

On the other hand, the small and eroded ectocuneiform AMNH 129996 (appendix 2, table 6) fits well with the slender MtIII described below. It is practically as broad as long, and its distal facet has a well-marked lateral entrant.

6. METAPODIALS: Three different metapodials are characterized by their relatively small size and slender proportions (fig. 17). They are eroded, especially at the distal epiphysis.

McII AMNH 129995 is similar in size to that from the juvenile of *H. tungurense* (AMNH 129956), but the former is already an adult and it differs in the McIII facet,

which is little developed both anteriorly and posteriorly. Being also a slender bone, its gracility index is somewhat greater, since with a similar transverse diameter of the diaphysis it is much shorter than the adult specimens of *H. tungurense* (appendix 2, table 7).

MtIII AMNH 129993 is long and narrow (appendix 2, table 7), with the diaphysis rectangular in section, and relatively thick. The proximal facet seems to be more regularly outlined than in *A. zernowi*, but its limits are badly preserved. It is rather slender, with hardly enlarged distal epiphysis.

MtIV AMNH 129994 is coincident with the anterior MtIII based on its size and slenderness. Its epiphyses are badly preserved, although the proximal tuberosity is well developed.

Discussion

It is not easy to determine the affinities of the bones in this group, but they seem to correspond to two different forms: one represented by the large scaphoids and ectocuneiform, and the other represented by the astragalus, calcaneum, navicular, small ectocuneiform, and metapodials. This second group recalls taxa referred to "*Dicerorhinus*" in morphology.

Chinese remains ascribed to *Dicerorhinus* come from the middle Miocene site of Jiulongkou (*D. cixianensis*) and the late Miocene sites of Bahe, Yushe, Qingyang (*D. orientalis*), and Duodaoshi (*D. ringstroemi*) (Li et al., 1984; Qiu, 1990). Following Qiu (1990), *D. cixianensis* is close to *Lartetotherium sansaniense* in both size and morphology. In turn, *D. orientalis* has been previously compared to *L. schleiermacheri*, a species classically included in *Dicerorhinus* and recently included in the genus *Lartetotherium* (Cerdeño, 1995).

The Tung-gur remains are smaller than the type material of *L. sansaniense* (personal data) but larger than the Spanish populations of this species (Cerdeño, 1986, 1989). In addition, the astragalus from Tung-gur shows a relatively narrower trochlea, and the MtIII is relatively less thick (APD) in its proximal epiphysis.

PHYLOGENETIC ANALYSIS

Taxa involved in this study have been analyzed through cladistic methodology, based on the previous analysis of the family Rhinocerotidae (Cerdeño, 1995). The data matrix, encompasing 48 taxa and 72 characters, is presented in appendix 3 (see op. cit.: table 2 for characters). The analysis discovered 780 equally parsimonious trees with a length of 485 (consistency index = 22; retention index = 60). Figure 18 presents the strict consensus tree of these 780. It shows two large polytomies (nodes 57 and 65) involving the groups of taxa under study, where the species level has been used. The unresolved clades do not provide good support for the relationships among these species. However, some statements can be made. Concerning the acerathere taxa, it is clear that Tung-gur type A is very close to *A. zernowi*, *A. depereti*, and *A. tsaidamense*, and that all of them are very close to "*H.*" *tetradactylum*. On the contrary, "*A.*" *paleosinense* appears to be much closer to *Chilotherium*, which supports its removal from the genus *Acerorhinus*. With respect to the iranotherines, Tung-gur type B appears related to the other genera. *Gobitherium* appears equally related to them, but only supported by dental characters (see Discussion). When *Gobitherium* is excluded from the analysis, Tung-gur type B appears closer to *H. lintungensis*.

The character states considered for the cladistic analysis do not seem to be sufficiently useful at a specific level, because differences among species are often subtle. For instance, all of the discussed acerathere species have long nasals and a high occiput, but differences among them exist within these character states.

BIOCHRONOLOGICAL AND ENVIRONMENTAL REMARKS

According to Qiu (1990), other Chinese localities of the same faunal level as Tung-gur (fig. 19) are Erlanggang, Fangxiang (Yan, 1979), and Linyanshan, Nanjing (Bi et al., 1977), where the rhinocerotids *Tesselodon fangxianensis* and *Diceratherium* sp. were recorded, respectively. Qiu et al. (1988a) stated the identity of the Asian "*Diceratherium*" with the genus *Acerorhinus*

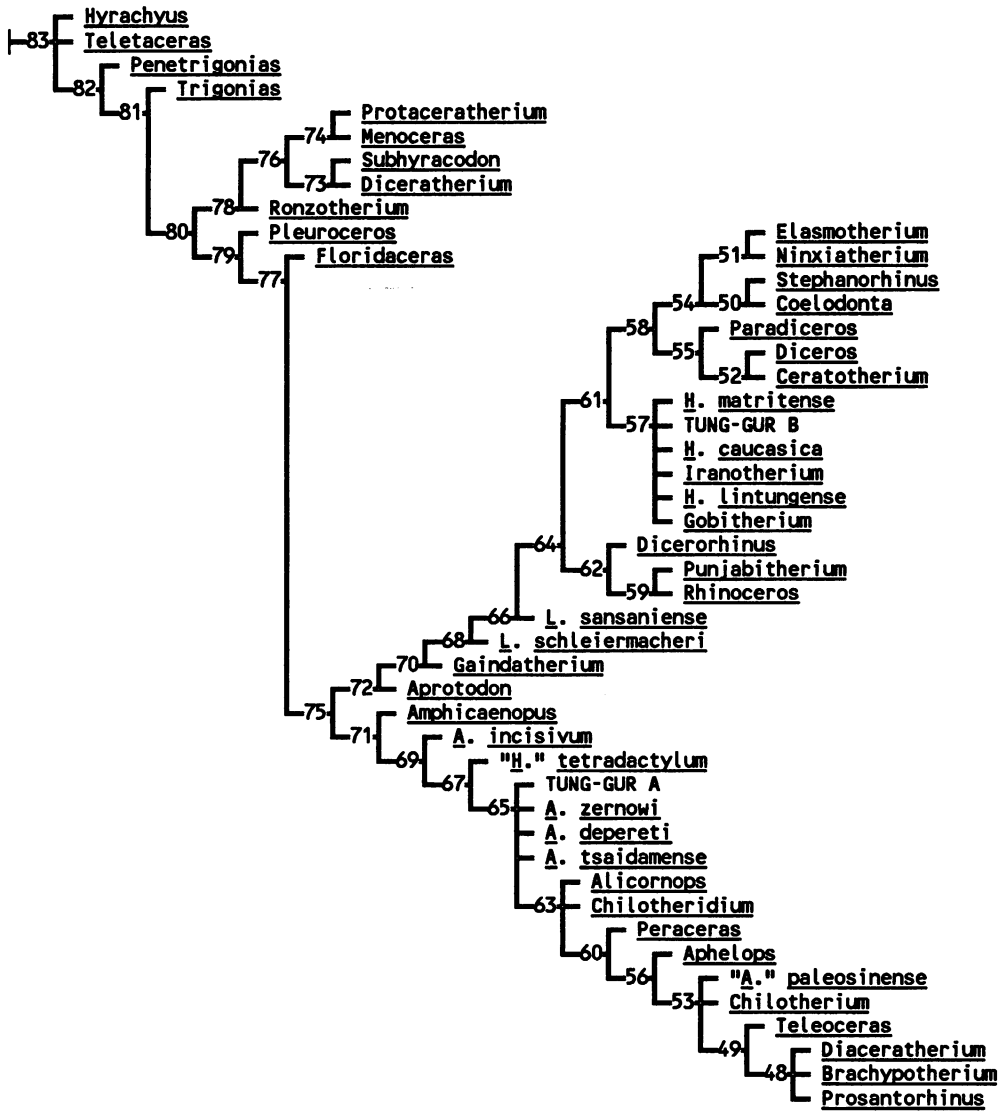

Fig. 18. Strict consensus tree of the 780 cladograms obtained for the family Rhinocerotidae, with *Hyrachyus* as outgroup.

Kretzoi, 1942, following Heissig (1975), who considered it to be a subgenus of *Chilotherium*.

The iranotherine species from the Chinese middle Miocene appear within three different faunal assemblages: the Tongxin (with "*Caementodon tongxinensis*"), Lengshuigou (with *Hispanotherium lintungensis*), and Tung-gur faunas, which are supposed to be successive in age (Li et al., 1984; Qiu, 1990) and are correlated with MN 5-6 to MN 7-8 of the European mammal chronology. Qiu (1990) stated that the Tongxin fauna is very close to that of Bielometchetskaya (Kuban, Caucasus), which includes *Hispanotherium caucasica* (Borissiak, 1938; Iñigo and Cerdeño, in press).

Ninxiatherium longirhinus was found at a locality of Zhongning County, Ningxia Hui region (Chen, 1977), and it was supposed to be late Miocene. Qiu (1990: 545, table 2) correlated Zhongning with the late Miocene

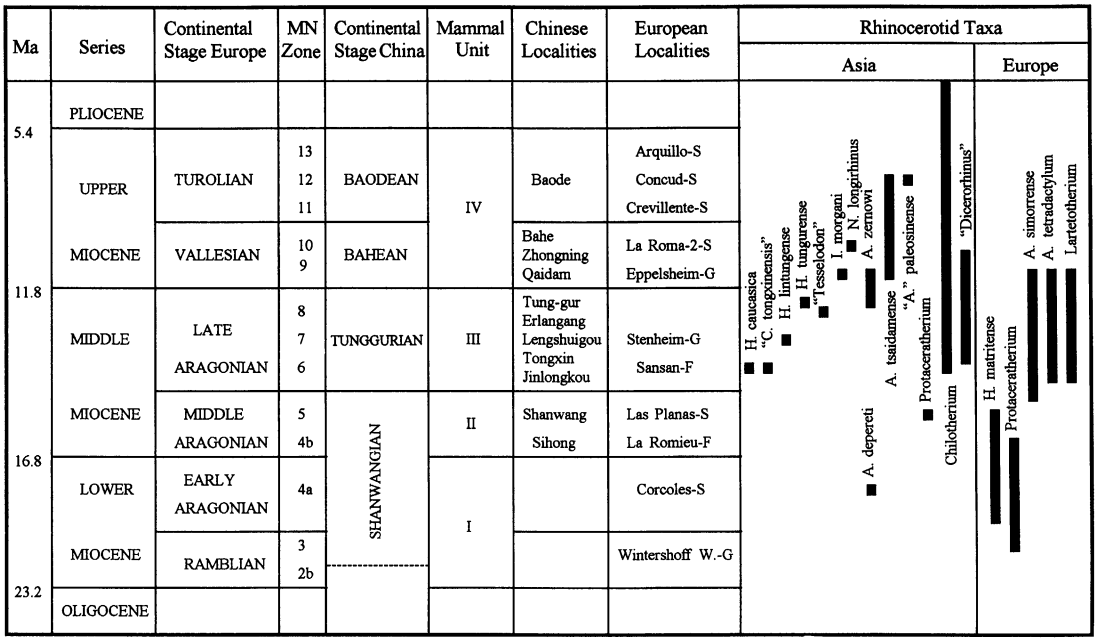

Fig. 19. Chronologic distribution of the rhinocerotid species included in this study.

Bahe fauna, and thus it is younger than Tung-gur. Guan and Zhang (1993a, 1993b) stated, however, that the fossiliferous bed of Zhongning corresponds to the late middle Miocene, although they did not refer to any rhinoceros species.

Hispanotherium tungurense, the latest representative of the genus in China, is roughly contemporary with the latest populations of *H. matritense* from Turkey (= *H. "grimmi"*; Heissig, 1976). The oldest record of the genus is *H. matritense* from the Spanish site of Córcoles (fig. 19), which is considered to be early Aragonian or MN 4a (Iñigo and Cerdeño, in press). Its Asian origin always accepted, the arrival of *Hispanotherium* on the Iberian Peninsula was suggested to have occurred through a Mediterranean island bridge (Antunes, 1979; Ginsburg and Antunes, 1979). That migration path, however, is not well supported by either paleontological data or paleogeographic reconstructions, although the alternative pathways are not supported either (Azzaroli, 1990). The age of Córcoles implies an older migration than previously thought (Iñigo and Cerdeño, in press). The record of *Hispanotherium* in France (Ginsburg et al., 1987) is younger than in Spain, from whence it would have migrated (Cerdeño, 1989).

The Tung-gur faunal level, placed at the end of the middle Miocene, may include the latest appearance of the genus *Hispanotherium*, although other iranotherines are present during the late Miocene (*Ninxiatherium*, *Iranotherium*).

The *Acerorhinus* lineage ranges from the early middle Miocene (middle Shanwangian) to the late Miocene (middle Baodean) (fig. 19). The presence of *Acerorhinus zernowi* in the late Tunggurian of Tung-gur implies an extension of its temporal range, since the type locality, Sebastopol, corresponds to the early Bahean (fig. 19). This suggests a migration wave from East Asia to the west.

The Chinese Miocene "dicerorhinine" forms are recorded from the middle to late Miocene, late Tunggurian to lower Bahean (Qiu, 1990).

Compared with the European Miocene faunas, both the acerathere and the "dicerorhinine" groups have their corresponding representatives through the middle to late Miocene: the former with *Alicornops*, "*Hoploaceratherium*," and *Aceratherium*, and

the latter with *Lartetotherium*. On the contrary, *Hispanotherium* disappeared from the European record by the late Aragonian. Its extinction has been correlated with environmental changes (Cerdeño and Nieto, 1995) when dry and warm conditions became wetter and cooler in the central Spanish basins. Its longer survival in Portugal and France, as well as its coexistence with other rhinocerotid species, has also been related to less severe climatic conditions (Cerdeño and Nieto, 1995; Iñigo and Cerdeño, in press).

Both *Aceratherium* and *Dicerorhinus* (sensu lato) have been recorded at different sites of the Caspian Sea area, through the Miocene (Gabunia, 1981). One iranotherine species, *Hispanotherium caucasica* (Borissiak, 1938; Iñigo and Cerdeño, in press), is known from the middle Miocene of Bielometchetskaya, whose faunal complex is assigned to a humid habitat (Gabunia, op. cit.).

The faunal turnover between the middle and the late Miocene Chinese faunal assemblages implies an increase of browsing mammal taxa, with rhinos as main elements among them. This is interpreted to indicate an important change in the vegetation (Kretzoi, 1987). The lesser representation of the iranotherines during the late Miocene (*Ninxiatherium*), in contrast to the presence of *Acerorhinus* and "dicerorhinines," supports a decrease of the grasslands.

ACKNOWLEDGMENTS

I especially thank Dr. R. H. Tedford for all the facilities provided during my stay in the AMNH. I am also grateful to Drs. M. C. McKenna, R. H. Tedford, M. T. Alberdi, C. Guérin, Z. Qiu, S. Roig, and E. Ortiz-Jaureguízar for their critical reading of the manuscript and their useful comments. This research has been possible thanks to a Fulbright fellowship within research projects PB91-0082 and PB94-0071, DGICYT, Spain.

REFERENCES

Antunes, M. T.
1979. *Hispanotherium* fauna in Iberian middle Miocene; its importance and paleogeographical meaning. Ann. Geol. Pays Hellen. VII Int. Congr. Mediterr. Neogene, Athens: 19–26.

Antunes, M. T., and L. Ginsburg
1983. Les rhinocérotidés du Miocène de Lisbonne—systématique, écologie, paleobiogéographie, valeur stratigraphique. Cienc. da Terra (UNL) 7: 17–98.

Azzaroli, A.
1990. Palaeogeography of terrestrial vertebrates in the perityrrhenian area. Palaeogeogr. Palaeoclimatol. Palaeoecol. 77: 83–90.

Beliajeva, E. I.
1971. Uber einige Nashörner, familie Rhinocerotidae, aus dem Neogen Westlinchen Mongolei (russ.). Fauna Mesozoja i Kajnozoja Zapadnoj Mongolii 3: 78–97.

Bi, Z., Z. Yu, and Z. Qiu
1977. First discovery of mammal remains from the upper Tertiary deposits near Nanking. Vertebr. Palasiat. 15(2): 126–138.

Bohlin, B.
1937. Eine Tertiäre Säugetier-Fauna aus Tsaidam. Paleontol. Sin. 14(1): 1–111.

Borissiak, A.
1914. Mammifères fossiles de Sebastopol. I. Mem. Comité Géol. 87: 154 pp.
1915. Mammifères fossiles de Sebastopol. II. Ibid., 137: 45 pp.
1927. *Aceratherium depereti* n. sp. from the Jilancik beds. Bull. Acad. Sci. URSS 21(6): 769–786.
1938. A new *Dicerorhinus* from the middle Miocene of North Caucasus. Trav. Inst. Paléozool. Acad. Sci. URSS 8(2): 1–69.

Cerdeño, E.
1986. El esqueleto postcraneal de *Lartetotherium sansaniense* (Mammalia, Rhinocerotidae). Estud. Geol. 42: 197–209.
1989. Revisión de la Sistemática de los rinocerontes del Neógeno de España. Colección Tesis Doctorales Nº 306/89. Edit. Univ. Complutense de Madrid: 429 pp., 64 t., 51 pl.
1992a. Spanish Neogene rhinoceroses. Palaeontology 35: 297–308.
1992b. New remains of the rhinocerotid *Hispanotherium matritense* at La Retama site: Tagus basin, Cuenca, Spain. Geobios 25(5): 671–679.
1993. Etude sur *Diaceratherium aurelianense* et *Brachypotherium brachypus* du Miocène Moyen de France. Bull. Mus. Natl. Hist. Nat. 15(1–4): 25–77.
1995. Cladistic analysis of the family Rhino-

cerotidae (Perissodactyla). Am. Mus. Novitates 3143: 25 pp.

Cerdeño, E., and M. Nieto
1995. Changes on western European Rhinocerotidae related to climatic variations. Paleoegeogr. Palaeoclimatol. Palaeoecol. 114: 325–338.

Chen, G.
1977. A new genus of Iranotheriinae of Ninxia [in Chinese]. Vertebr. Palasiat. 15(2): 143–146.

Colbert, E. H.
1939. A new anchitherine horse from the Tung-gur Formation of Mongolia. Am. Mus. Novitates 1019: 9 pp.

Crusafont, M., and J. F. de Villalta
1947. Sobre un interesante rinoceronte (*Hispanotherium*) del Mioceno del Valle del Manzanares. Ciencias 12: 869–883.

Farris, J. S.
1988. Hennig86, version 1.5. Computer program and documentation. Distributed by author, Port Jefferson Station, N.Y.

Fischer, G.
1809. Sur l'*Elasmotherium* et le *Trogontherium*. Mém. Soc. Imp. Nat. Moscou 2.

Fortelius, M., and K. Heissig
1989. The phylogenetic relationships of the Elasmotherini (Rhinocerotidae, Mammalia). Mitt. Bayer. Staatssamml. Paläontol. Hist. Geol. 29: 227–233.

Gabunia, L.
1981. Traits essentiels de l'évolution des faunes de Mammifères néogènes de la région mer Noire-Caspienne. Bull. Mus. Natl. Hist. Nat. 3: 195-204.

Ginsburg, L., and M. T. Antunes
1979. Les Rhinocérotidés du Miocène inférieur et moyen de Lisbonne (Portugal). Succession stratigraphique et incidences paléogéographiques. C. R. Acad. Sci. Paris 288: 493–495.

Ginsburg, L., and K. Heissig
1989. *Hoploaceratherium* n. gen., a new generic name for "*Aceratherium*" *tetradactylum*. In: D. R. Prothero and R. M. Schoch (eds.), The evolution of perissodactyls, 418–421. New York: Oxford Univ. Press.

Ginsburg, L., F. Maubert, and M. T. Antunes
1987. Découverte d'*Hispanotherium* et de *Gaindatherium* (Rhinocerotidae, Mammalia) dans le Miocène de France. Bull. Mus. Natl. Hist. Nat. 9(3): 303–311.

Guan, J.
1993. Primitive elasmotherines from the middle Miocene, Ningxia (northwestern China). Mem. Beijing Nat. Hist. Mus. 53(12): 200–207.

Guan, J., and X. Zhang
1993a. The middle Miocene lithic and mammalian records from Ningxia and Lazhong basins, northwestern China. Mem. Beijing Nat. Hist. Mus. 53(12): 229–236.
1993b. The middle Miocene mammals from Guanghe and Hezheng in northwestern China. Mem. Beijing Nat. Hist. Mus. 53(12): 243–251.

Guérin, C.
1980. Les rhinocéros (Mammalia, Perissodactyla) du Miocène terminal au Pleistocène supérieur en Europe occidentale. Comparaison avec les espèces actuelles. Doc. Lab. Géol. Lyon 79: 1182 pp.

Heissig, K.
1972. Paläontologische und geologische Untersuchungen im Tertiär von Pakistan; 5: Rhinocerotidae aus den unteren und mittleren Siwalik-Schichten. Abh. Bayer. Akad. Wiss. Math. Naturwiss. Kl. 152: 1–112.
1974. Neue Elasmotherini (Rhinocerotidae, Mammalia) aus dem Obermiozän Anatoliens. Mitt. Bayer. Staatssamml. Paläontol. Hist. Geol. 14: 21–35.
1975. Rhinocerotidae (Mammalia) aus dem jungtertiär Anatoliens. Geol. Jahrb. 15: 145–151.
1976. Rhinocerotidae (Mammalia) aus der *Anchitherium*-Fauna Anatoliens. Geol. Jahrb. 19: 1–121.

Huang, W., and D. Yan
1983. New material of Elasmotherini from Shennongjia, Hubei. Vertebr. Palasiat. 21(3): 223–229.

Iñigo, C.
1993. Estudio de los Perisodáctilos del yacimiento Mioceno de Córcoles (Guadalajara). Doctoral thesis, Univ. Complutense de Madrid, 559 pp.

Iñigo, C., and E. Cerdeño
In press. The *Hispanotherium matritense* (Rhinocerotidae) from Córcoles (Guadalajara, Spain): its contribution to the systematics of the Miocene Elasmotherini. Geobios.

Kretzoi, M.
1942. Bemerkungen zum System der nachmiozänen Nashorn-Gattungen. Földt. Közl. 72: 309–318.
1943. *Gobitherium* n. g. (Mammalia, Rhinocerotidae). Ibid., 73: 268–271.
1987. Remarks on the correlation between European and Asian late Cenozoic lo-

cal biostratigraphies. Vertebr. Palasiat. 25(2): 146-157.

Li, C., W. Wu, and Z. Qiu
1984. Chinese Neogene: subdivision and correlation. Vertebr. Palasiat. 22(3): 171–178.

Osborn, H. F.
1924. *Serridentinus* and *Baluchitherium*, Loh Formation, Mongolia. Am. Mus. Novitates 148: 5 pp.

Osborn, H. F., and W. Granger
1932. *Platybelodon grangeri*, three growth stages, and a new serridentine from Mongolia. Am. Mus. Novitates 537: 13 pp.

Pavlow, M.
1914. Mammiferes tertiaires de la nouvelle Russie. 2 partie. *Aceratherium incisivum*, *Hipparion*, Proboscidea, Carnivora. Moscou: Soc. J. N. Kouchnereff et Cie.

Prado, C. de
1864. Descripción física y geológica de la provincia de Madrid. Junta General de Estadística, 219 pp.

Qiu, Z.
1990. The Chinese Neogene mammalian biochronology—its correlation with the European Neogene mammalian zonation. *In*: E. H. Lindsay, V. Fahlbusch, and P. Mein (eds.), European Neogene mammal chronology, 527–556. New York: Plenum Press.

Qiu, Z., J. Xie, and D. Yan
1988a. A new chilothere skull from Hezheng Gansu, China—with special reference to the Chinese "*Diceratherium*." Sci. Sin. 31(4): 493–502.

Qiu, Z., D. Yan, G. Chen, and Z. Qiu
1988b. Preliminary report on the field work in 1986 at Tung-gur, Nei Mongol. Kexue Tongbao (Sci. Bull.) 33(5): 399–405.

Ringström, T.
1924. Nashörner der *Hipparion*-fauna Nord-Chinas. Paleontol. Sin. 1(4): 1–159.

Yan, D.
1979. Several species of fossil mammals from the Miocene of Fangxian County, Hubei Province. Vertebr. Palasiat. 17(3): 189–199.

Yan, D., and K. Heissig
1976. Revision and autopodial morphology of the Chinese-European rhinocerotid genus *Plesiaceratherium* Young 1937. Zitteliana 14: 81–109.

Zhai, R.
1978. A primitive Elasmothere from the Miocene of Lintung, Shensi. Prof. Pap. Strat. Paleontol. 7: 122–126.

APPENDIX 1

Abbreviations Used in Text and Tables

ant.	anterior
APD	anteroposterior diameter
APDB	APD at beak level
APDDA	APD at distal articulation
APDI	APD at internal side
APDMAX	maximal APD
APDPR	proximal APD
APDT	APD tuber
art.	articular
D/d	upper/lower milk molar (D indicates diagonal in upper teeth)
DA	distal articulation
dis.	distal
DL	distance between lips of trochlea
epi.	epiphysis
H	height
HANT	anterior height
HART	articular height
HCON	condyle height
HM1M2	horizontal ramus height between M1 and M2
HMAX	maximal height
HMIN	minimal height
HOCC	height occipital crest–condyle
HP4M1	horizontal ramus height between P4 and M1
HZIG	posterior height of zygomatic arch
I/i	upper/lower incisor
j.	juvenile
L	length
l.	left
Lab	absolute length
Lan	anatomical length
LICO	length nasal incision–condyle
LINT	length of nasal incision
LIOC	length nasal incision–occipital crest
LIOR	length nasal incision–orbit
LNCO	length nasal–occipital condyle
LNOC	length nasal–occipital crest
LpS-C	length posterior symphyseal border–condyle
LS-C	length symphysis–condyle
LS-T	length symphysis–mandibular angle
LSYMP	symphyseal length
M/m	upper/lower molar
max.	maximal
min.	minimal
P/p	upper/lower premolar
post.	posterior
proc.	process
prox.	proximal
r.	right
TD	transverse diameter
TDANT	anterior TD
TDAPO	TD apophysis
TDDA	TD distal articulation
TDM	maximal TD
TDMD	maximal distal TD
TDP	posterior TD
TDS	TD at sustentaculum level
TDT	TD tuber
trans.	transverse
W	width
WCOC	width of occipital crest
WCON	width of each condyle
WFRO	frontal width
WM1M2	horizontal ramus width between M1 and M2
WMOC	maximal occipital width
WNAS	nasal width
WOCON	width at occipital condyles
WP4M1	horizontal ramus width between P4 and M1
WSYMP	symphyseal width
WZIG	zygomatic width

APPENDIX 2

TABLE 1

Dimensions of Skulls and Mandibles from Tung-gur

	LNOC	LNCO	LIOC	LICO	LIOR	LINT	WZIG	WFRO	WNAS	WOCON	HOCC	HZIG	WCOC	WMOC
Skull														
26215, A	567.5	590.0	420.0	440.0	82.7	169.4	287.0	202.7	78.2	115.0	222.0	58.6	120.4	230.0
26520, A	495.0	530.0	370.0	390.0	70.8	143.0	293.0	172.4	78.8		220.0	54.2	112.0	
26522, A						153.1		171.4	63.4					
26220, A					87.5		310.0	190.0		134.5	233.5	68.0	115.0	240.0
26531, B					139.4	131.0			117.4			64.2		
26521, j.B	550.0	530.0	440.5	430.0	118.3	103.6	230.0	139.3	65.5	116.7	180.7	44.6	118.3	159.2

	LS-C	LpS-C	LSYMP	LS-T	WSYMP	WCON	HCON	WP4M1	HP4M1	WM1M2	HM1M2
Mandible											
26222, A	484.0	375.0	136.0		92.6	114.4	240.8	49.0	76.6	51.9	85.8
26221, A						104.6	248.5	45.9	84.6	41.9	91.0
26525, A			121.0	495.0		104.9		44.6	67.8	41.6	75.7
26218, A						105.8	252.8	42.6		43.7	87.4
26215, A	521.8	421.0	134.9	518.0		109.8	220.0	43.3	73.4	44.1	85.1
26526, B			78.9	466.0				44.3	75.5	48.8	77.3
26217, B								52.3	84.8	57.2	99.1
26540, B								61.4	72.8	60.2	82.6

TABLE 2
Dimensions of Teeth from Tung-gur

	L P1	W P1	L P2	W P2	L P3	W P3	L P4	W P4	L M1	W M1	L M2	W M2	L M3	W M3	D M3
Upper teeth															
26523, A							43.0	53.9	47.7	52.2	51.7	53.5	46.6	50.6	53.3
129858, A											57.7	64.0	53.8	55.4	59.4
26215, A	25.7	21.1	31.8	39.8	38.1	51.2	43.1	57.5	48.4	57.9	53.2	59.3	47.8	51.2	54.8
26215, A	25.1	20.0	31.9	39.0									44.8	50.2	47.9
26520, A							41.6	51.2	50.3	55.7	49.6	55.0	45.6	47.1	53.0
26530, B	20.5	18.1	26.2	30.5	34.2	41.8	36.2	47.2	48.9	59.2	60.9	63.5	46.4	59.8	63.4
26531, B							36.1	53.1	42.5	64.4	64.0	70.6	60.0	67.5	69.5
26531, B							39.4	57.9			64.6	73.1			68.7
26577, B													50.6	56.6	61.1
Upper milk teeth															
26532, B	24.7	19.2	27.1	28.7	33.4	32.7	42.3	35.3	48.9	(38.8)					
26532, B	24.5	22.2	30.3	27.3	31.8	33.5	42.0	38.7	49.2						
26542, B	27.7	21.2	33.0	31.1	40.9	40.1	46.4	41.0							

	L P1	W P1	L P2	W P2	L P3	W P3	L P4	W P4	L M1	W M1	L M2	W M2	L M3	W M3
Lower teeth														
26221, A							35.3	30.2	39.6		40.9	28.4	41.0	27.1
26222, A					31.3	23.6	33.5	27.3	38.7	28.7	38.9	29.2	41.8	28.2
26525, A					32.9	25.1	36.4	30.6	40.4	31.2	42.7	29.7	44.8	27.5
26525, A					34.2		37.4	30.9	40.9		43.0	30.3		28.7
26218, A			28.3	17.5	37.5	26.9	39.1	28.9	43.3	30.0	46.7	30.0	42.4	26.4
26214, A			25.2	17.9	32.3	22.8	37.1	27.7	41.5	28.9	44.4	27.1	39.7	23.1
26216, A			25.5	19.6	35.9		38.3	29.5	43.4	30.9	44.3		45.0	29.1
26527, A							37.6	26.6	43.6	28.7	44.2	28.5		
26215, A	9.9	8.9	26.9	18.0	33.4	23.1	36.9	26.1	40.3	30.9	43.9	28.2	49.0	28.2
26215, A	12.6	8.1	29.1	18.5	33.4	23.9	37.2	25.4	40.8					
26578, B			25.2	17.9	31.6	21.7	30.6	23.7	41.9	27.5				
26217, B							37.6	30.2	41.8	34.6	57.5	35.5	60.6	36.7
26541, B					31.9	23.2	31.6	25.1	41.1	29.3	48.6	27.3	46.6	25.7
26540, B			29.2	19.2	29.2	22.9	33.9	27.2	41.9	34.4	54.8	35.8	51.8	32.9
26528, B					27.7		29.8	30.2	(31.9)	(33.5)	46.7	38.8	55.2	34.7
26528, B								33.7			44.3	39.0	55.8	36.9
Lower milk teeth														
129916, A	10.6	6.8	28.0	15.4	35.0	19.9	37.9	22.1						
129943, B					(28)	16.0	32.4	17.3						
26521, B	18.5	9.3	29.3	18.1	36.9	22.3	41.1	23.8	50.4	23.8				
26521, B			28.7	16.6	35.9	20.6	40.6	22.5	48.7	22.5				
26533, B			24.4	15.8	33.7	21.5	38.9	26.0	41.7	25.6				
26529, B	10.5	7.4	24.3	15.3	33.6	19.9	36.8	21.6	41.8	21.9				
26529, B	11.0	7.7	24.7	15.9	33.3	19.0	36.3	22.2	40.9	22.2				
26537, B	15.7	10.1	27.8	19.3	35.1	22.8	39.1	28.4	54.3					
26537, B	14.8	9.4	27.4	17.9	35.9	24.1	38.1	25.5	46.5	27.5				

TABLE 3
Dimensions of Long Bones from Tung-gur

		Prox. expi.		Prox. art.		Diaphysis		Dis. epi.		Dis. art.	
	L	TD	APD	TD	APD	TD	APD	TD	APD	TD	APD
Humerus											
26215, A						58.2	67.1	126.4	104.2	88.2	78.2
26215, A						57.7	61.1	124.6	110.8	86.6	77.6
129840, A	375.0	138.9	120.1	81.5	72.5	49.2	53.4	111.0	93.3	84.0	71.1
Radius											
129837, A	317.5	87.3	55.5	84.6	44.8	49.5	38.5	90.3	62.2	80.7	42.2
26215, A	320.6	86.1	50.6	79.2	41.6	46.5	37.1	90.2	60.6	79.5	37.1
26215, A		82.8	52.1	78.2	41.5	46.8	38.7				
129838, A	293.3	83.2	52.6	77.8	43.5	42.0	34.5		(52)		(35)
Ulna											
26215, A	406.4	59.7	81.6	77.8		40.7	36.5		51.7	27.4	28.4
26215, A	395.0	53.8	76.9	75.7		40.1	38.4				
Femur											
26215, A	(493)			77.3	(72)	65.9	55.6	123.9	152.4	102.3	70.0
129945, B	(464)			89.9		63.5	51.7	135.8	166.4	(119)	78.5
Tibia											
129839, A	344.0	118.6	93.7			49.6	47.2	87.4	68.5	62.0	54.9
129841, A	326.0	109.2	96.5			52.4	51.6	86.4	62.9	63.4	50.7
129831, A	328.0	103.5	99.7			58.1	43.6	83.3	65.9	66.7	51.7
129946, B	(391.5)					56.6	51.1	93.5	76.9	74.3	64.6
Fibula											
26215, A	298.9	27.9	31.5			15.0	24.6	24.1	42.1		
26215, A	298.6	29.9	41.1			16.5	25.5	27.1	46.4	33.3	24.0
129946, B	(345)					13.3	14.7	19.3	43.0	34.9	21.0

TABLE 4
Dimensions of Patellae from Tung-gur

	H	TD	APD
Patella			
26215, A	88.4	82.3	42.9
129890, A?	83.3	76.6	42.0

TABLE 5
Dimensions of Carpal Bones from Tung-gur

					Prox. art.		Dis. art.	
	APD	TD	HMAX	HANT	APD	TD	APD	TD
Scaphoid								
129831, A	71.0	44.5	60.9	52.5	44.7	39.0	59.0	26.5
129925, A	70.4	44.9	58.9	49.7	43.6	40.6	57.0	30.7
129926, A	66.7	41.6	53.1	46.0	42.9	38.9		22.9
129927, A	66.4	44.3	53.3	45.5	40.7	40.5	46.9	29.1
129928, A	64.8	39.8	48.5	43.6	40.7	39.2	51.1	22.7
129942, A	61.1	38.9	50.6	40.0	36.2	37.3	51.2	25.9
129991, ?				53.5				33.5
129990, ?		47.4	72.3		50.0	45.7		34.0
129974, B	71.3		(52)	50.0	(42)		(54)	28.3

	APD	TD	HMAX	HANT
Semilunate				
129831, A	65.9	46.7	46.1	48.0
129835, A	59.2	(33)	39.0	41.0
129845, A	62.6	44.2	46.8	47.8
129975, B	66.7	49.6	50.2	53.4
Pisiform				
129831, A	61.5	22.7	39.1	24.4
129961, B	67.1	24.9	46.4	30.9
129978, B	65.4	23.6	46.3	30.2

	APD	TD	H	APDPR
Pyramidal				
26581a, A	39.7	36.6	47.5	24.4
129889, A	40.2	39.6	50.6	30.8
129929, A	35.9	38.5	52.4	30.2
129846, A	35.2	40.7	53.1	30.3
129977, B	42.9	41.4	49.4	33.6
129976, B	41.3	40.8	49.6	34.3
129960, B	46.0	40.9	51.9	32.0
129969, B	43.7	41.8	47.2	33.1
129970, B	47.0	40.7	(51)	35.7
129967, j.B	34.0		(41)	28.2

	APD	TD	HMAX	HMIN
Trapezoid				
129915, A	33.4	22.7	26.8	19.2
129891, A	36.5	24.9	31.4	23.0
129892, A	35.0	24.4	29.1	21.1
129971, B	47.3	27.2	33.6	23.7

	APD	TD	HMAX	HART	APDDA	TDDA
Magnum						
129893, A	78.5	37.8	51.6	51.2	44.1	31.7
129979, B	88.6	41.8	61.9	58.3	44.3	38.2

TABLE 5—(*Continued*)

	H	TD	Lab	Lan
Unciform				
129831, A	45.1	56.1	77.1	65.6
129930, A	43.4	54.3	73.3	60.5
129931, A	42.1	54.0	74.2	56.0
129833, A	41.3	51.7	66.9	48.9
129836, A	40.1	52.1	74.2	55.7
129894, A	43.3	54.7	73.9	63.9
129973, B	48.9	60.8		
129972, B	45.4	63.6		
129854, j.B	38.7	46.4	59.3	45.8

TABLE 6

Dimensions of Tarsal Bones from Tung-gur

	TDM	HMAX	TDDA	APDDA	TDMD	DL	APDI
Astragalus							
129909, A	78.9	71.5	67.8	40.9	67.7	49.6	55.5
129910, A	71.8	67.9	63.8		65.2	48.2	52.3
129911, A	72.2		60.3		64.5	48.4	43.8
129852, A	78.9	68.6	62.4	34.8	68.1	46.6	50.6
129933, A	82.4	68.7	70.4	37.2	76.5	48.7	50.4
129934, A	79.3	71.5	66.1		69.2	52.6	
129935, A	73.0	62.5	61.3		68.4	50.3	50.4
129831, A	78.1	68.7	62.9	38.0	66.2	49.5	48.9
129895, A	76.2	70.2	69.1	43.1	69.1	48.6	47.5
129986, ?	78.7	76.8	72.3	45.0	73.7	50.8	51.0
129989, ?	88.5	79.5	71.8	43.1	75.6	53.7	53.2
129980, B	83.9	76.2	68.3	41.8	71.4	53.2	50.4

	HMAX	TDT	APDT	TDS	APDB	TDP
Calcaneum						
129831, A	107.6	42.8	61.3	68.2	53.1	35.8
129907, A	109.0	42.2	58.9	67.8	56.8	36.4
129908, A	107.7	45.3	65.4		58.0	35.8
129923, A	111.7	46.9	60.3	58.6	54.9	34.9
129924, A	99.9	42.9	57.5	66.3	51.0	35.7
129897, A	107.1	40.6	64.5	61.5	56.3	32.2
129898, A	104.5	42.1	54.1	56.4	51.0	31.6
129849, A	97.9	39.3	56.0		54.0	31.0
129848, A	102.5	57.8	62.1	67.4	50.9	38.4
129987, ?	114.5	40.1	57.5	60.3	54.4	27.8
129982, B	122.0	44.3	61.6		61.7	32.1
129981, B	122.7	47.4	65.6	68.4	60.7	35.8

TABLE 6—(*Continued*)

					Prox. art.		Dis. art.	
	APD	TDANT	HMAX	HANT	APD	TD	APD	TD
Cuboid								
129831, A	62.4	32.0	47.7	39.6	36.5	31.8	35.0	29.8
129932, A	55.7	32.2	48.4	37.6	34.1	32.3	29.9	27.9
129834, A	58.0	33.4	54.7	38.1	32.3	36.5	32.5	28.3
129847, A	62.3	34.7	52.1	37.7	40.5	34.5	33.8	33.0
129894, A	65.7	39.3	58.7	39.7	41.6	35.4	31.1	35.4
129949, B	67.2	39.7	57.7	45.3	(41)	32.6	39.2	35.0
129963, B	70.4	41.7	62.1	44.6	51.9	42.3	39.9	36.5
129964, B	58.6	32.6	45.5	40.4	39.2	33.6	38.0	29.5
	APD	TD	HMAX	HMIN				
Navicular								
129831, A	54.3	41.2	26.8	18.4				
129832, A	52.1	42.1	26.5	20.3				
129988, ?	59.3	40.5	31.0	23.2				
129983, B	52.7	43.2	(27)	20.9				
129966, B	62.4	47.1	29.0	24.5				
Ectocuneiform								
129996, ?	38.7	39.0	21.2	17.9				
129992, ?	55.1	52.2	30.8	23.3				
129984, B	45.9	52.2	23.2	17.8				
Mesocuneiform								
129831, A	27.5	(20)	13.9	12.4				
	APDMAX	APDPR	TDPR	TDAPO	HMAX	HMIN		
Entocuneiform								
129914, A?	31.9	21.0	14.9	15.1	43.1	33.0		

TABLE 7
Dimensions of Metapodials from Tung-gur

		Prox. epi.		Prox. art.		Diaphysis		Dis.	Dis. art.		Gracility
	L	TD	APD	TD	APD	TD	APD	TD	TD	APD	index
McII											
129955, B	177.0	28.5	41.1	22.3	37.8	30.6	16.3	36.8	33.0	37.6	17.28
129954, B	180.0	35.6	46.2	29.3	41.5	36.2	19.3	43.4	36.1	39.2	20.11
129953, B	172.0	32.1	42.2	24.9	39.8	34.2	18.3	37.6	32.7	37.1	19.88
129956, j.B	(150)	27.8	39.4	24.8	30.0	27.2	14.0	(35)			
129995, ?	146.0	27.9	36.4	20.4		30.1	15.2	32.6	27.6	31.7	20.61
McIII											
129831, A		52.9	42.5	51.6	42.6	45.2	19.2				
129918, A	168.5	50.9	43.9	48.5	41.8	44.0	19.3	61.2	50.4	42.7	26.11
129855, A	166.0	55.2	45.8	52.4	43.1	44.6	20.3	50.4	51.0	43.0	26.86
129899, A	152.1	53.9		50.8		41.5	17.5	51.5			27.28
129900, A	150.2	49.9		45.1		39.3	19.6	53.5	45.0	38.1	26.16
129901, A	146.1	44.6	37.9	42.5	34.2	40.3	16.5	49.2	43.9	36.7	27.58

TABLE 7—(*Continued*)

		Prox. epi.		Prox. art.		Diaphysis		Dis.	Dis. art.		Gracility
	L	TD	APD	TD	APD	TD	APD	TD	TD	APD	index
129856, A	159.8	51.7	40.6	48.7	38.8	39.7	16.9	52.5	47.5	40.0	24.84
129857, A	151.1	47.0	37.8	44.4	37.4	38.1	13.6	>45.5	41.2	38.1	25.21
129951, B	195.0		48.7		46.9	42.8	23.1	54.5	49.3	45.7	21.94
129952, B	190.8	56.2	41.1	52.9	40.8	40.6	21.8	52.7	47.1	40.5	21.27
McIV											
26215, A	134.7	35.5	36.7	29.1	32.9	29.4	16.3	34.5	34.1	33.0	21.82
129922, A	124.9	36.1	37.6	30.2	31.9	29.8	16.7	37.6	35.2	34.4	23.85
129921, A	126.1	32.1	35.9		32.0	25.0	13.9	34.5	31.3	35.5	19.82
129957, B	164.9	41.3	42.6	35.7	39.2	29.9	20.3	36.5	33.5	37.2	18.13
129958, B	(162)					33.6	21.7	45.7	40.5	39.0	(20.74)
MtII											
129902, A	125.0	25.1	36.4	18.8		21.5	19.6	31.0		35.8	17.20
129903, A	126.8	28.8	41.3	17.9	29.8	25.0	19.9	33.3	33.7	36.5	19.70
129913, A	122.1	25.2	37.5	18.8	32.2	28.4	20.8	33.3	33.4	37.8	23.20
129920, j.A	114.0	22.3	33.4	17.6	25.7	22.0	15.5	29.1	28.6	33.7	19.30
MtIII											
129904, A	141.8	39.0	38.9	35.4	34.2	36.8	18.0	46.8	43.6	36.2	25.95
129912, A	137.2	39.9	36.4	38.5	32.9	38.1	16.0	49.6	44.5	34.1	27.76
129919, j.A	129.0	37.5				36.9	16.9	46.7	40.8	36.0	28.60
129993, ?	147.8	40.3	33.9	37.7	32.1	33.8	19.2	43.9	37.6		22.86
MtIV											
129894, A	138.1	40.6	40.2	30.6	37.4	24.5	22.3	30.1	29.6	38.7	17.7
129994, ?	132.1	33.9	29.8	26.3	23.4	22.6	18.8		23.1	27.7	17.1

TABLE 8

Dimensions of Phalanges from Tung-gur

	TD	APD	H
1st central			
129831, A	42.8	31.4	33.4
129906, A?	41.5	31.6	30.6
129894, A	49.7	35.2	36.8
129905, A	49.5	34.6	33.9
129962, B	47.3	34.8	40.9
129965, B	48.1	35.0	43.5
1st lateral			
129894, A	37.6	38.7	35.6
129968, B	41.0	41.7	39.3
2nd lateral			
129894, A	35.1	29.7	25.8

APPENDIX 3

Data Matrix Including *Hyrachyus,* as Outgroup, 47 Rhinocerotid Taxa, and 72 Characters

Character / Taxa	1234	56789	11111 01234	11111 56789	22222 01234	22222 56789	33333 01234	33333 56789	44444 01234	44444 56789	55555 01234	55555 56789	66666 01234	66666 56789	777 012
Hyrachyus	0000	00000	00000	00000	00000	00000	00000	00000	11210	00000	20100	00010	10000	00000	000
Teletaceras	0000	00000	00000	10000	00000	011?0	0000?	00000	01000	010??	??0??	0?0??	?0???	?1???	??0
Penetrigonias	0000	000?0	0?000	10010	00110	0?110	0100?	?00?0	02110	00???	?????	0?010	10010	1????	1??
Amphicaenopus	0000	10001	11110	01110	0111?	01200	01002	00100	0222?	001??	20???	?????	?????	??00?	0?0
Trigonias	0000	10000	01000	11000	00110	01100	0100?	00100	022?0	01000	201?0	10010	?00?0	11???	???
Subhyracodon	0000	?000?	?0000	00000	01110	01110	01112	?0100	0?000	0?010	21?10	00010	?0010	11000	100
Diceratherium	0200	0000?	01000	11000	01110	01110	01112	200?0	00000	01010	21010	00010	?1000	01000	010
Menoceras	0100	10002	22000	11001	01111	11100	01112	20120	01100	01011	30010	00010	11000	11000	110
Floridaceras	0000	?01?0	??0?0	11100	01111	11200	01012	20010	02120	00100	00110	10101	00100	01100	101
Peraceras	0000	11000	0?011	01?11	01111	13210	11012	211?0	01001	11200	10?10	10111	?1??0	1???1	10?
Aphelops	0000	1100?	12101	?1101	11111	13210	11011	112?0	00101	10100	10000	11021	01000	?1011	101
Teleoceras	1000	2000?	?2111	?1111	11111	02211	21111	112?0	02221	02310	10210	21121	?2000	11110	101
Ronzotherium	0000	10001	?1100	11?0?	01110	11100	01011	10000	01??0	00001	?1210	000?0	11?11	??00?	1?1
Protaceratherium	0000	0100?	00000	11010	11111	01100	01112	11120	01???	00000	31010	00110	11??0	11000	?10
Pleuroceros	0200	20001	10100	11000	?1111	01100	01?11	10?10	??011	00010	0?0?0	10000	?1101	0????	??0
Diaceratherium	1000	20002	?0211	11101	01111	02200	01012	22210	00???	11300	?0210	211?1	0210?	11101	001
Brachypotherium	1000	10002	10211	01111	01111	02200	11012	22210	002?1	11310	?0200	211?1	????1	11101	001
Prosantorhinus	1000	10000	1??0?	11011	01111	01210	01112	22220	0011?	00300	?0210	211?1	01000	11101	001
Alicornops	0000	11000	10100	11111	11111	01210	01012	20210	01101	01200	?0010	211?1	00110	11000	101
"H." tetradactylum	0000	11000	10000	11110	11111	13200	01012	20210	01111	00100	11010	10120	010?1	0100?	000
TUNG-GUR A	0000	2100?	?0000	11111	11111	?32?0	01012	20210	02??1	?01?0	??010	11120	?1?11	01001	000
A. zernowi	0000	2100?	12000	11111	?1111	??210	01012	20110	02211	00???	?????	?????	?????	??00?	???
"A." depereti	0000	21000	01000	1111?	?1111	03?10	01012	20210	02001	0000?	?????	1?1??	????1	0?001	?00
A. tsaidamense	0000	11000	11000	11?11	11111	03210	01112	20210	?2??1	0?1??	1????	????0	110?1	01??0	?10
"A." paleosinense	0000	01001	00100	01101	11111	13210	?1?11	21220	12121	00???	?2???	?????	?????	?????	???
A. incisivum	0000	11002	20000	01110	11111	?2200	01011	10210	02221	00100	1?010	101?0	010?1	0100?	?00
Chilotherium	0000	01002	10211	01211	11111	13210	21111	?1210	22221	0?310	??010	11121	?10??	??111	?01
Chilotheridium	2000	11002	01000	1100?	?1111	13210	21?12	20210	10??1	00100	??010	1?1??	0111?	1???0	?01
Aprotodon	0000	?????	2110?	112??	?1111	?12?0	1111?	10210	02??0	012??	20200	20010	11000	10??1	?01
L. sansaniense	2010	10000	10100	11001	1111?	01100	01102	21110	22221	00111	20211	10100	11010	00??1	?00
L. schleiermacheri	2010	10001	22000	11010	?1110	01110	01102	201?0	22221	00111	20201	10100	11010	1?001	101
Stephanorhinus	2011	21?12	21100	11000	11111	13310	?1102	21120	?2??1	0?111	20?01	10100	1100?	1?001	?0?
Coelodonta	2012	11?12	21100	1102?	21111	13310	20012	21120	22221	12111	20201	10100	11??1	00001	001
H. matritense	2000	?00??	????0	11000	1111?	0?110	11101	11221	?22?1	02011	20000	101?0	11011	01?00	110
TUNG-GUR B	2000	10012	01000	11000	?1111	131?0	11101	12111	22221	020?0	20?01	10111	110?1	11??0	??0
H. caucasica	2000	?00??	?????	11000	1111?	03110	11?01	11221	22221	0201?	00000	10120	110?1	11000	110
H. lintungense	2000	1001?	???00	11???	?1111	?????	111??	12?11	22???	?2???	?????	?????	?????	?????	???
Iranotherium	2000	10112	01000	11000	01111	0???0	11?01	12221	2222?	021??	?????	101??	?????	?????	???
Elasmotherium	0022	11112	00200	1102?	21111	1331?	21101	12222	2222?	02110	?????	101??	?????	?????	?01
Ninxiatherium	2001	11212	00100	?1???	?1111	?3???	11?0?	11221	2222?	?2???	?????	?????	?????	?????	???
Gobitherium	0000	?000?	????0	10???	?111?	?????	1??0?	12221	22???	?2???	?????	?????	?????	?????	???
Gaindatherium	2000	10002	20000	11110	01110	11200	01102	20000	22220	0011?	?????	?????	?????	?????	???
Punjabitherium	2010	20002	22100	1100?	?1110	01110	211?2	21120	22???	?21??	?????	?????	?????	?????	???
Rhinoceros	2000	20002	22101	1110?	01111	01110	?1112	21110	?2221	02111	00101	10101	10001	01111	001
Dicerorhinus	2010	00002	00100	11000	11111	?1110	01102	20010	22221	01111	0?101	001?0	?0000	10111	1?1
Diceros	2010	20002	01200	11021	21111	13310	01112	20010	02221	01111	11101	10101	00000	10111	?01
Ceratotherium	2010	10002	01100	1102?	21111	13310	21112	20010	22221	12111	11101	10101	10000	01111	001
Paradiceros	2010	10002	00100	11021	?1111	13310	01112	21110	12??1	0??11	?????	0?1??	?????	??10?	??0

Recent issues of the *Novitates* may be purchased from the Museum. Lists of back issues of the *Novitates, Bulletin,* and *Anthropological Papers* published during the last five years are available free of charge. Address orders to: American Museum of Natural History Library, Department D, Central Park West at 79th St., New York, N.Y. 10024. TEL: (212) 769-5545. FAX: (212) 769-5009. E-MAIL: scipubs@amnh.org